JCI The Journal of Clinical Investigation

# Hepatic fibrosis, glomerulosclerosis, and a lipodystrophy-like syndrome in PEPCK-TGF-beta1 transgenic mice.

D E Clouthier, … , S A Comerford, R E Hammer

*J Clin Invest.* 1997;100(11):2697-2713. https://doi.org/10.1172/JCI119815.

**Research Article**

Transgenic mice overexpressing a constitutively active human TGF-beta1 under control of the rat phosphoenolpyruvate carboxykinase regulatory sequences developed fibrosis of the liver, kidney, and adipose tissue, and exhibited a severe reduction in body fat. Expression of the transgene in hepatocytes resulted in increased collagen deposition, altered lobular organization, increased hepatocyte turnover, and in extreme cases, hemorrhage and thrombosis. Renal expression of the transgene was localized to the proximal tubule epithelium, and was associated with tubulointerstitial fibrosis, characterized by excessive collagen deposition and increased fibronectin and plasminogen activator inhibitor-1 immunoreactivity. Pronounced glomerulosclerosis was evident, and hydronephrosis developed with low penetrance. Expression of TGF-beta1 in white and brown adipose tissue resulted in a lipodystrophy-like syndrome. All white fat depots and brown fat pads were severely reduced in size, and exhibited prominent fibroplasia. This reduction in WAT was due to impaired adipose accretion. Introduction of the transgene into the ob/ob background suppressed the obesity characteristic of this mutation; however, transgenic mutant mice developed severe hepato- and splenomegaly. These studies strengthen the link between TGF-beta1 expression and fibrotic disease, and demonstrate the potency of TGF-beta1 in modulating mesenchymal cell differentiation in vivo.



# Hepatic Fibrosis, Glomerulosclerosis, and a Lipodystrophy-like Syndrome in PEPCK-TGF-β1 Transgenic Mice

**David E. Clouthier, Sarah A. Comerford, and Robert E. Hammer**
*Department of Biochemistry and the Howard Hughes Medical Institute, University of Texas Southwestern Medical Center, Dallas, Texas 75235-9050*

## Abstract

**Transgenic mice overexpressing a constitutively active human TGF-β1 under control of the rat phosphoenolpyruvate carboxykinase regulatory sequences developed fibrosis of the liver, kidney, and adipose tissue, and exhibited a severe reduction in body fat. Expression of the transgene in hepatocytes resulted in increased collagen deposition, altered lobular organization, increased hepatocyte turnover, and in extreme cases, hemorrhage and thrombosis. Renal expression of the transgene was localized to the proximal tubule epithelium, and was associated with tubulointerstitial fibrosis, characterized by excessive collagen deposition and increased fibronectin and plasminogen activator inhibitor-1 immunoreactivity. Pronounced glomerulosclerosis was evident, and hydronephrosis developed with low penetrance. Expression of TGF-β1 in white and brown adipose tissue resulted in a lipodystrophy-like syndrome. All white fat depots and brown fat pads were severely reduced in size, and exhibited prominent fibroplasia. This reduction in WAT was due to impaired adipose accretion. Introduction of the transgene into the *ob*/*ob* background suppressed the obesity characteristic of this mutation; however, transgenic mutant mice developed severe hepato- and splenomegaly. These studies strengthen the link between TGF-β1 expression and fibrotic disease, and demonstrate the potency of TGF-β1 in modulating mesenchymal cell differentiation in vivo. (*J. Clin. Invest.* 1997. 100:2697–2713.) Key words: TGF-β1 • liver • kidney • adipose tissue • differentiation**

## Introduction

The TGF-β superfamily constitutes a diverse group of structurally related polypeptides whose members are potent modulators of cell proliferation and differentiation. TGF-β1, the prototype of the family, has numerous pleiotropic functions, including inhibition of epithelial and induction of mesenchymal cell proliferation, inhibition of mesenchymal cell differentiation, stimulation of extracellular matrix (ECM)[1] synthesis and deposition, regulation of pericellular proteolytic activity, cytokine stimulation, chemoattraction, angiogenesis induction, and immunosuppression (1).

TGF-β1 is secreted as a latent polypeptide that is proteolytically cleaved after homodimerization at a cluster of basic residues to yield the biologically active peptide. The biological actions of TGF-β1 are elicited through binding of the mature active form of the molecule to specific cellular receptors present on the surface of all normal and most neoplastic cells, three of which have been identified. TGF-βs signal through ligand-dependent heterotetromeric complexes of type I (TβR-I) and type II (TβR-II) transmembrane receptor serine/threonine kinases (2). Ligand binding to TβR-II recruits and phosphorylates TβR-I, which in turn propagates the signal to downstream intracellular targets, some of which have been identified through their direct physical association with either of the receptors in yeast two-hybrid screens. The most definitive information regarding signaling directly from the receptor complex has come from studies on a family of related proteins identified on the basis of their homology to the *Drosophila mad* protein and to the *Caenorhabditis elegans sma-1, -2 and -3* genes (3, 4). Of the five vertebrate genes identified, Smad-2/MADR2, Mad-3/Smad-3/hMAD-3, and Smad-4/h-Mad-4/DPC-4 are specifically involved in TGF-β signaling. Signaling appears to involve phosphorylation of one of the Smads by the TβR-I kinase, its obligate association with Smad-4/h-Mad-4/DPC-4, followed by translocation of the DPC-4/Smad complex to the nucleus, leading to transcriptional transactivation of TGF-β target genes (3, 4).

TGF-β plays an important role in wound healing, a complex but orderly process that involves implementation and coordination of many of its specific functions. It promotes tissue stabilization after damage through increased synthesis of ECM components such as collagen and fibronectin, increased integrin expression, and rapid induction of protease inhibitors such as plasminogen activator inhibitor-1 (PAI-1), ensuring deposition and maintenance of an intact matrix (5). Wound repair, however, unless controlled, can result in fibrosis, a state typified by inappropriate proliferation of mesenchymal cells and accumulation of ECM, leading to impaired function and ultimate destruction of normal organ architecture. A number of pathological conditions such as arthritis, idiopathic pulmonary fibrosis, scleroderma, and keloids, all possess characteristics in-

D.E. Clouthier and S.A. Comerford contributed equally to this work.

Address correspondence to Robert E. Hammer, Department of Biochemistry, and the Howard Hughes Medical Institute, University of Texas Southwestern Medical Center, Dallas, TX 75235-9050. Phone: 214-648-5026; FAX: 214-648-7607; E-mail: hammer@utsw.swmed.edu David E. Clouthier's present address is Department of Molecular Genetics and the Howard Hughes Medical Institute, University of Texas Southwestern Medical Center, Dallas, TX 75235.

*Received for publication 3 June 1997 and accepted in revised form 30 September 1997.*

J. Clin. Invest.

0021-9738/97/12/2697/17 $2.00
Volume 100, Number 11, December 1997, 2697–2713
http://www.jci.org

1. *Abbreviations used in this paper:* BAT, brown adipose tissue; BrdU, bromodeoxyuridine; ECM, extracellular matrix; LPL, lipoprotein lipase; PAI-1, plasminogen activator inhibitor-1; PEPCK, phosphoenolpyruvate carboxykinase; WAT, white adipose tissue.

dicative of fibrosis, and are associated with increased TGF-β1 expression (6). Such inappropriate expression and its consequences have led to excessive TGF-β1 action being referred to as the dark side of tissue repair (7).

Two organs of particular clinical interest with respect to fibrotic disease are the liver and kidney. Hepatic fibrosis is strongly associated with increased TGF-β1 expression in chronic liver diseases such as chronic hepatitis and alcoholic cirrhosis (8). Increased renal expression of TGF-β1 is also a hallmark of glomerulonephritis and diabetic nephropathy, conditions generally characterized by excessive accumulation of ECM within the mesangium of the glomeruli, leading to a decreased filtration rate, proteinuria, hypertension, and ultimately organ failure (9).

In addition to its effects on matrix deposition, TGF-β1 is also a potent modulator of cellular proliferation and differentiation. While inhibition of epithelial cell proliferation is mediated by its effects on cell cycle progression through the G1-S boundary (10), its effects on differentiation are illustrated by its ability to block myogenic and adipogenic differentiation in vitro (11–13). As the pericellular environment is capable of providing instructive signals for induction and progression of differentiation (14–16), it is possible that TGF-β1 mediates these inhibitory effects on differentiation through its effects on ECM synthesis (5).

To investigate the ability of TGF-β1 to regulate cell proliferation and differentiation in vivo, and to evaluate its role in the pathogenesis of fibrosis, we have used a transgenic approach. We have targeted the expression of a constitutively active TGF-β1 molecule to liver, kidney, and white (WAT) and brown (BAT) adipose tissue using the regulatory sequences of the rat phosphoenolpyruvate carboxykinase gene (PEPCK; EC 4.1.1.32) (17).

In multiple lines, targeted expression of the transgene caused severe fibrotic disease. Fibrosis of the liver occurred with varying degrees of severity depending upon the level of TGF-β1 expression. Other liver phenotypes associated with expression of the transgene included hemorrhage, thrombosis, hepatocyte apoptosis, and a mild increase in hepatic mass. Overexpression of the transgene in kidney also resulted in fibrosis and glomerular disease, eventually leading to complete loss of renal function. Severe obstructive uropathy (hydronephrosis) was also observed in a number of animals. Expression of TGF-β1 in adipose tissue resulted in a dramatic reduction in total body WAT and a marked, though less severe, reduction in BAT. This reduction in WAT mass was due to impaired development. These findings confirm in vivo that aberrant TGF-β1 expression can cause severe organ damage and failure through complications resulting from fibrosis, and can profoundly influence cellular differentiation programs.

## Methods

*Mutagenesis of TGF-β1 cDNA.* Mutagenesis was performed in two stages according to the method of Hemsley et al. (18). Plasmid pGEM4/TGF-β1 containing a full-length 1.45-kb human TGF-β1 cDNA (provided by Dr. Randall Moreadith, Ryburn Cardiology Center, University of Texas Southwestern Medical Center), was digested with KpnI and BamHI to isolate a 490-bp fragment encompassing amino acids 145–310. This fragment was subcloned into plasmid pSP73 (Promega Corp., Madison, WI), which was then used as a template for PCR amplification using the following oligonucleotides: 5′ AGCGCCCACAGCTCCTGTGA 3′ and 5′ AAGGCGAAAGCCCTCAATTT 3′ to introduce a mutation from T to A at nucleotide 794. PCR was carried out over 25 cycles using a thermal cycler and the following conditions: 94°C, 1 min; 50°C, 2 min; 72°C, 3 min (Perkin Elmer Corp., Norwalk, CT). The 2.95-kb amplified linear product was visualized on a 0.9% low melting point agarose gel, eluted, and treated with Klenow fragment and polynucleotide kinase to permit recircularization with T4 ligase. Sequencing of the product confirmed incorporation of the correct mutation. This plasmid then served as template for a second round of mutagenesis using oligonucleotides 5′ CACAGCTCCAGTGACAGCA 3′ and 5′ GGCGCTAAGGCGAAAGC 3′ to introduce a mutation at nucleotide 800. Sequencing of this amplified product confirmed incorporation of the correct mutation to yield a mutated fragment with cysteines 223 and 225 undergoing conversion to serines. The mutated 490-bp KpnI-BamHI fragment was subcloned into the backbone of TGF-β1 to create a full-length 1.45-kb mutated cDNA. Generation of a mature, biologically active mutant TGF-β1 molecule was confirmed by expression in COS cells, and by assaying culture medium for active TGF-β1 in the MuMLV inhibition assay (19).

*Gene construction and generation of transgenic mice.* To create the PEPCK-TGF-β1 fusion gene, the mutant TGF-β1 (Ser223/225) was removed from the plasmid pSP70-TGF-β1 by restriction with EcoRI. pECE, a plasmid containing the 5′ and 3′ untranslated regions from SV40 (20), was digested with EcoRI, and the ends were dephosphorylated using calf intestinal alkaline phosphatase (Boehringer Mannheim Biochemicals, Indianapolis, IN). The mutant TGF-β1 cDNA was shuttled into pECE, generating the plasmid peTGF-β1, which contained the 1.45-kb TGF-β1 cDNA fused to the 3′ untranslated region of SV40. This fragment was liberated by restricting peTGF-β1 with BglII and SphI, and ligating into BglII-SphI–digested pePEPCK, a plasmid containing 2,100 bp of the promoter and 5′ sequences of the rat PEPCK gene. The resulting plasmid, pePEPCK-TGF-β1, was digested with SspI and SphI to yield a 4.2-kb fragment containing the complete PEPCK-TGF-β1 fusion gene. The transgene was separated from vector sequences by agarose gel electrophoresis and recovered by electroelution using the Little Blue Tank (Isco, Inc., Lincoln, NE). The purified fragment was injected into the pronuclei of fertilized one-cell (C57Bl/6 × SJL) F2 mouse eggs, which after culturing to the two-cell stage, were transferred to the oviduct of day 1 pseudopregnant B6CBAF1/J recipients. Transgenic mice were identified by dot blot analysis of DNA isolated from a tail biopsy using either a $^{32}$P-labeled 1.45-kb EcoRI TGF-β1 cDNA probe, or a 0.65-kb BamHI–XbaI fragment encompassing the SV40 polyA region from plasmid pGEM-SV40 (provided by Dr. D. Ornitz, University of Washington, St. Louis). Lines 334-4, 335-5, and 339-4 were established and maintained by breeding to C57Bl/6 × SJL F1 hybrid animals. Lines 332-4 and 340-1 were initially established through ovarian transplants and maintained by breeding to hybrid animals.

*Generation and genotyping of TGF-β transgenic ob/ob mice.* To place the TGF-β1 transgene onto the *ob/ob* background, ovaries from *ob/ob* females (Jackson Laboratory, Bar Harbor, ME) were transplanted to the ovarian bursa of C57Bl/6 × SJL F1 recipients, and the females were bred to transgenic males from line 340-1. Transgenic TGF-β:*ob*/+ males were mated to the *ob/ob* ovarian recipients, and the resulting progeny were genotyped for the ob mutation by PCR amplification of a portion of the leptin gene, followed by DdeI digestion of the amplified product. The C-T transition at nucleotide 428 in the mutant leptin cDNA creates a new DdeI site that is absent in the wild-type leptin gene (21). The leptin-specific oligonucleotide primers used were 5′-ATTCTGAGTTTGTCCAAGATGGACC-3′ (5′ oligo) and 5′-CCACTGGTCTGAGGCAGGGAGCAGC-3′ (3′ oligo) with 34 cycles of amplification as follows: 95°C, 2 min; 58°C, 30 s; 72°C, 30 s, followed by a 10-min extension at 72°C. DdeI digestion of the amplified product resulted in 2 fragments of 108 and 47 bp (mutant *ob* allele) or an uncleaved 155-bp fragment (wild-type *ob* allele). Products were visualized on a 3.5% agarose gel (MetaPhor; FMC Bioproducts, Rockland, ME).

*RNA analysis by Northern blot hybridization.* Total cellular RNA was extracted from tissues using the guanidinium thiocyanate-cesium chloride procedure (22). 12 μg RNA was denatured at 50°C with glyoxal for 1 h before separating on a 1.5% agarose gel in 10 mM $NaPO_4$ buffer (pH 7.0) using a vertical gel apparatus (CBS Scientific, Del Mar, CA). Transfer of RNA to Nytran (Schleicher and Schuell, Inc., Keene, NH) was allowed to proceed overnight, and the filter was baked at 80°C for 2 h under a vacuum.

Hybridizations using cDNA probes were performed as previously described (23). Human TGF-β1 mRNA was detected with the entire 1.45-kb human TGF-β1 cDNA from the plasmid pSP70-TGF-β1. The 2.1-kb C/EBP-α probe was provided by Dr. Dan Lane (Johns Hopkins University School of Medicine), and the 1.4-kb LPL probe was provided by Dr. Michael Schotz (University of California, Los Angeles). Final washes were carried out at 0.1 × SSPE (15 mM NaCl, 1 mM $NaH_2PO_4$, 0.1 mM EDTA), 0.5% SDS at 65°C, and the blots were exposed to XAR-5 film with intensifying screens at −80°C for 6–18 h.

Prehybridizations and hybridizations with a $^{32}P$ end-labeled 18S oligonucleotide probe 5′ GCCGTGCGTACTTAGACATGCATG 3′, derived from nucleotides 50–73 of the rat 18S ribosomal RNA gene sequence were carried out as previously described (23). Final washes were done in 6× SSC at 37°C. Blots were exposed to XAR-5 film (Eastman Kodak Co., Rochester, NY) with intensifying screens at −80°C for 0.5–2 h. Radioactivity on the filters was quantitated by phosphorImager analysis using a PhosphorImager with a radioanalytic imaging instrument (Molecular Dynamics, Sunnyvale, CA).

*Histology and immunohistochemistry.* Tissues prepared for routine histological examination including hematoxylin and eosin staining, Masson's trichrome staining, which reveals collagen (24), and Gordon and Sweet's method for revealing reticular fibers (24), were fixed in 10% neutral-buffered formalin, embedded in paraffin, and sectioned at 5 μm. Tissues used for immunohistochemical analysis were isolated from animals that were intracardially perfused with 4% paraformaldehyde. Tissues were immersion-fixed for an additional 6–12 h in 4% paraformaldehyde, dehydrated in a graded series of ethanols, embedded in paraffin, and sectioned at 5 μm. Sections were mounted on poly-L-lysine–coated glass slides, baked at 56°C for 30 min, deparaffinized in xylene, and rehydrated through graded alcohols. Endogenous peroxidase activity was quenched by incubating sections in 0.3% hydrogen peroxide in methanol for 30 min and rinsing in PBS. For polyclonal primary antibodies, nonspecific binding was blocked using serum of the species from which the secondary antibody was raised. Sections were incubated with primary antibody overnight at 4°C and with secondary antibody for 1 h at room temperature. For monoclonal antibodies, sections were incubated in 0.01% avidin to block endogenous biotin activity after hydrogen peroxide treatment. After rinsing in PBS, sections were blocked in horse serum (15%) followed by indirect immunocytochemistry using the reagents and suggested protocols of the Mouse IgG Vectastain ABC Elite kit (Vector Laboratories, Inc., Burlingame, CA). Sections were incubated with primary antibody for 1 h at room temperature. The secondary antibody used was biotinylated horse anti–mouse IgG (30 μg/ml) supplied in the ABC kit.

Sheep antihuman fibronectin (used at 30 μg/ml) was obtained from The Binding Site (San Diego, CA), turkey antihuman TGF-β1 (40 μg/ml) was obtained from Collaborative Biomedical Products (Bedford, MA), and a monoclonal antibody against human plasminogen activator inhibitor-1 (PAI-1; 2 μg/ml) was obtained from American Diagnostica, Inc. (Greenwich, CT). Biotinylated rabbit anti–chicken/turkey IgG (15 μg/ml) was obtained from Zymed Laboratories, Inc. (South San Francisco, CA) and biotinylated rabbit anti–sheep IgG (15 μg/ml) was obtained from Vector Laboratories, as was normal horse and rabbit serum. For all immunohistochemical staining, aminoethyl carbamazole (Zymed Laboratories, Inc.) was used as the chromagen, and methyl green (Sigma Chemical Co., St. Louis, MO) was used for counterstaining. Controls included the incubation of both primary and secondary antibodies with tissues isolated from nontransgenic animals, and the omission of primary and secondary antibodies on sections from transgenic tissue.

*Measurement of cell proliferation.* A single intraperitoneal injection of bromodeoxyuridine (BrdU, 100 μg/g body weight; Sigma Chemical Co.) was given 2 h before death. Tissues were removed, immersed in Carnoy's fixative for 4 h, transferred to 100% ethanol, blocked in paraffin, and sectioned at 5 μm. BrdU incorporation into cells undergoing S-phase DNA synthesis was detected using a biotinylated monoclonal antibody to BrdU, streptavidin peroxidase, and DAB substrate according to manufacturer's instructions (Calbiochem Corp., San Diego, CA).

*In situ detection of oligonucleosomal DNA fragmentation.* Detection of cells undergoing apoptosis was performed using a modified terminal dUTP nick end labeling (TUNEL) assay (25) on 5-μm-thick sections from formalin-fixed, paraffin-embedded tissue using direct fluorescent (flourescein) detection of digoxygenin-11-dUTP/dATP–labeled genomic DNA. All reagents used were constituents of the Apoptag kit (Oncor Inc., Gaithersburg, MD).

*DNA quantitation.* Weighed tissue was placed in SNET buffer (20 mM Tris, pH 8.0, 5 mM EDTA, 1% SDS, 400 mM NaCl) and subjected to Proteinase K digestion (0.2 mg/ml) for 8 h at 55°C with agitation. DNA was phenol:chloroform extracted, and the concentration was determined by measuring the fluorescence of bisbenzimide H33258 (26) using a Perkin Elmer fluorimeter. Ultrapure calf thymus DNA (Sigma Chemical Co.) was used as a standard.

*Proximate analysis.* 7-mo-old transgenic and control littermate males from line 340-1 (Table I) were subjected to proximate analysis to determine total body fat composition (Nutrition International, Dayton, NJ). Animals were killed, and carcasses were frozen, homogenized, and chemically analyzed for protein, fat, ash, crude fiber, and carbohydrate content. Fat content was specifically determined by extracting acid hydrolysates with equal volumes of ether and petroleum, and weighing the residue.

## Results

The PEPCK-TGF-β1 fusion gene was microinjected into the pronuclei of fertilized one-cell hybrid mouse eggs, and 32 transgenic founder mice were produced. Many founder mice were smaller than control littermates, and had lost the normal elasticity of trunk skin, making them difficult to restrain. Early morbidity of founders was observed, usually occurring before

*Table I. PEPCK-TGF-β1 Expression in Transgenic Mice*

| | | TGF-β1 mRNA* | | Primary phenotypes | | | | |
|---|---|---|---|---|---|---|---|---|
| Line | Transgene | Liver | Kidney | Liver | Kidney | WAT‡ | BAT§ | Skin‖ |
| | *copies/cell* | | | | | | | |
| 332-4 | 32 | ++ | +++ | Fl | GS/HN | S | ++++ | +++ |
| 334-4 | 3 | ++++ | + | F | GS | M | + | +/− |
| 335-5 | 21 | + | ++ | Fl | GS | S | | +++ |
| 339-4 | 48 | ++++ | ++ | F/Fl | GS | S | ++ | +++ |
| 340-1 | 10 | + | + | Fl | GS/HN | S | +++ | +++ |

F, fibrosis; Fl, fatty liver; GS, glomerulosclerosis; HN, hydronephrosis. *Liver and kidney TGF-β1 expression were assessed by RNA analysis. ‡Expression in epididymal white fat (WAT) was assessed by RNA analysis. Direct line comparisons were not made. The quantity of renal, inguinal, mesenteric, and mammary gland WAT was assessed macroscopically. Epididymal fat pads were weighed, and the relative reduction assessed as severe (S) or moderate (M). §Expression in BAT was assessed by RNA analysis; line comparisons were not made. The degree of fibrosis was assessed histologically. ‖The severity of the loss of skin elasticity was assessed by manually restraining the animals.

the animals reached sexual maturity. Necropsy of three of these mice revealed severe hemorrhage and thrombosis of the liver. Viable founder animals that expressed the transgene in liver were identified by analyzing liver total cellular RNA for TGF-β1 transcripts. To ensure maximal transgene expression, animals were fed a low-carbohydrate diet for 2 wk before partial hepatectomy (17). Founder animals were selected for generating lines on the basis of a high level of TGF-β1 transcripts in liver, and on the loss of elasticity of trunk skin. Eleven transgenic lines were established, five of which form the basis of this analysis. Animals in all five lines exhibited a common array of phenotypes, which included marked fibrosis of the liver, kidney, skin, and both WAT and BAT (Table I). Animals from four out of the five lines exhibited severe reduction in the size of both white and brown fat deposits. Expression of the transgene resulted in elevated circulating plasma levels of TGF-β that ranged from 18 to 50 ng/ml (control animals had a mean level of 6 ng/ml), and these levels were line-dependent. There were no apparent gross or histologic lesions in any other organs examined.

To establish the sites and to assess the tissue hierarchy of TGF-β1 expression, total cellular RNA was isolated from tissues known to express PEPCK from two representative transgenic lines (334-4 and 340-1), and then subjected to Northern analysis. The transgene was expressed at high levels in multiple organs, including liver, kidney, WAT, BAT, and portions of the gut (Fig. 1 *A*), a pattern of expression observed with other transgenes transcriptionally regulated by the rat PEPCK 5′ sequences (17). Other more minor sites of expression included skin, lung, and bladder (Fig. 1 *B*). While the cell specificity of TGF-β1 expression in these organs was not characterized, the presence of active human TGF-β1 in skin and bladder correlated with severe skin fibrosis and hydronephrosis (see Fig. 6 *A*). To determine if the levels of TGF-β1 expression in liver and kidney correlated with disease manifestations in these organs, we compared expression of the transgene across lines (Fig. 1, *C* and *D*). Expression of TGF-β1 in liver was moderate in three lines, and very high in the two lines (Fig. 1 *C*), which showed marked liver fibrosis (Table I). In the kidney, expression was more moderate and comparable in three of the five lines, and was less marked in two (Fig. 1 *D*). All of the lines, however, showed a similar severity of renal disease and fibrosis (Table I), suggesting that the lesions were, in part, due to blood-borne TGF-β and not only to local production.

Transcription of PEPCK and PEPCK-driven transgenes can be modulated, both positively and negatively, by altering the carbohydrate composition of the diet (17). To assess whether any of the lines of mice exhibited regulatable expression, age- and sex-matched transgenic animals from each line were placed on either a high- (suppressing) or low- (inducing) carbohydrate diet for 2 wk, and the liver was analyzed for TGF-β1 transcripts (Fig. 1 *E)*. Only animals from one of the four lines examined showed moderately regulatable expression of the transgene in liver, with the quantity of TGF-β1 transcripts in carbohydrate-fed animals being approximately sevenfold lower than in animals on the protein diet.

To establish the cell specificity and regional distribution of TGF-β1 expression in liver, immunohistochemistry was performed on liver from control and transgenic mice using a polyclonal anti–human TGF-β1 antibody. The livers of control mice exhibited TGF-β1 immunoreactivity in a uniform perisinusoidal distribution, and were excluded from parenchymal cells (Fig. 2 *A*). This pattern of distribution is identical to the pattern previously described for hepatic localization of TGF-β1 (27), and indicates cross-reactivity of the antibody with endogenous mouse TGF-β1. In the livers of transgenic mice, TGF-β1 immunoreactivity was also localized to sinusoidal endothelial cells; however, the most intense immunoreactivity was present in periportal hepatocytes diminishing towards central vein areas (Fig. 2 *B*). This regional pattern of distribution is consistent with known sites of PEPCK enzyme activity (28) and with the pattern of expression of reporter transgenes directed by the rat PEPCK 5′ regulatory sequences (17).

Chronic ectopic expression of active TGF-β1 in liver caused multiple hepatic lesions. The livers of transgenic mice with the highest levels of TGF-β1 transcripts (line 334-4) showed marked alterations in general liver organization and hepatocyte morphology (Fig. 2, *D, F,* and *H*). Cellular heterogeneity could be seen across the lobule with smaller more vacuolated hepatocytes in central areas. Enlarged hepatocyte nuclei were also commonly seen (Fig. 2, *D*, *F*, and *H*), suggesting either the persistence of senescent cells, which under normal circumstances would undergo programmed cell death, or cells arrested in G2 of the cell cycle (29, 30). In the most severe cases, there was a generalized swelling and crowding of hepatocytes such that sinusoidal fenestrations were obliterated (Fig. 2, *D* and *H*). To determine the extent and the magnitude of the fibrotic response to chronic hepatic TGF-β1 expression, we examined the livers of mice from line 334-4 for evidence of enhanced collagen deposition. Livers of control mice showed very little collagen deposition throughout lobules (Fig. 2 *E*). In contrast, the livers of transgenic mice showed marked collagen deposition localized to the sinusoids and around periportal areas (Fig. 2 *F*).

To determine if these morphologic changes were reflected in impaired liver function, we measured the serum levels of several markers of hepatocellular disease. An increase in the ratio of aspartate aminotransferase (AST) and alanine aminotransferase (ALT) is often indicative of hepatic disease (31). In transgenic mice of the 334-4 line, the AST:ALT ratio was approximately twofold higher than in age- and sex-matched littermates (data not shown). The serum levels of other parameters such as albumin and alkaline phosphatase were unaffected by expression of the transgene. Thus, the hepatic fibrosis that occurs in TGF-β1 transgenic mice is associated with a moderate impairment in liver function.

The normal adult liver is a relatively quiescent organ with little cellular turnover. To assess whether chronic expression of TGF-β1 in liver altered hepatocyte turnover, we examined the livers of transgenic and control mice for evidence of DNA synthesis and cell death. On gross examination, the livers of mice from the 334-4 line were larger ($\sim$ 13%) than normal, and on histologic examination consistently showed uneven edges, a morphologic feature indicative of a mild regenerative response (Fig. 2 *B*). Analysis of liver DNA content indicated that the modest increase in the size of the liver was primarily due to hypertrophy rather than hyperplasia (data not shown). BrdU labeling of control and transgenic lines, however, showed an approximately eightfold increase in the number of transgenic hepatocytes in S-phase, in contrast to a near absence of DNA synthesis in control animals (Fig. 3 *B*).

To determine to what extent hepatocytes from transgenic livers were undergoing apoptosis, livers from control and transgenic mice were processed for detection of nuclear oligo-

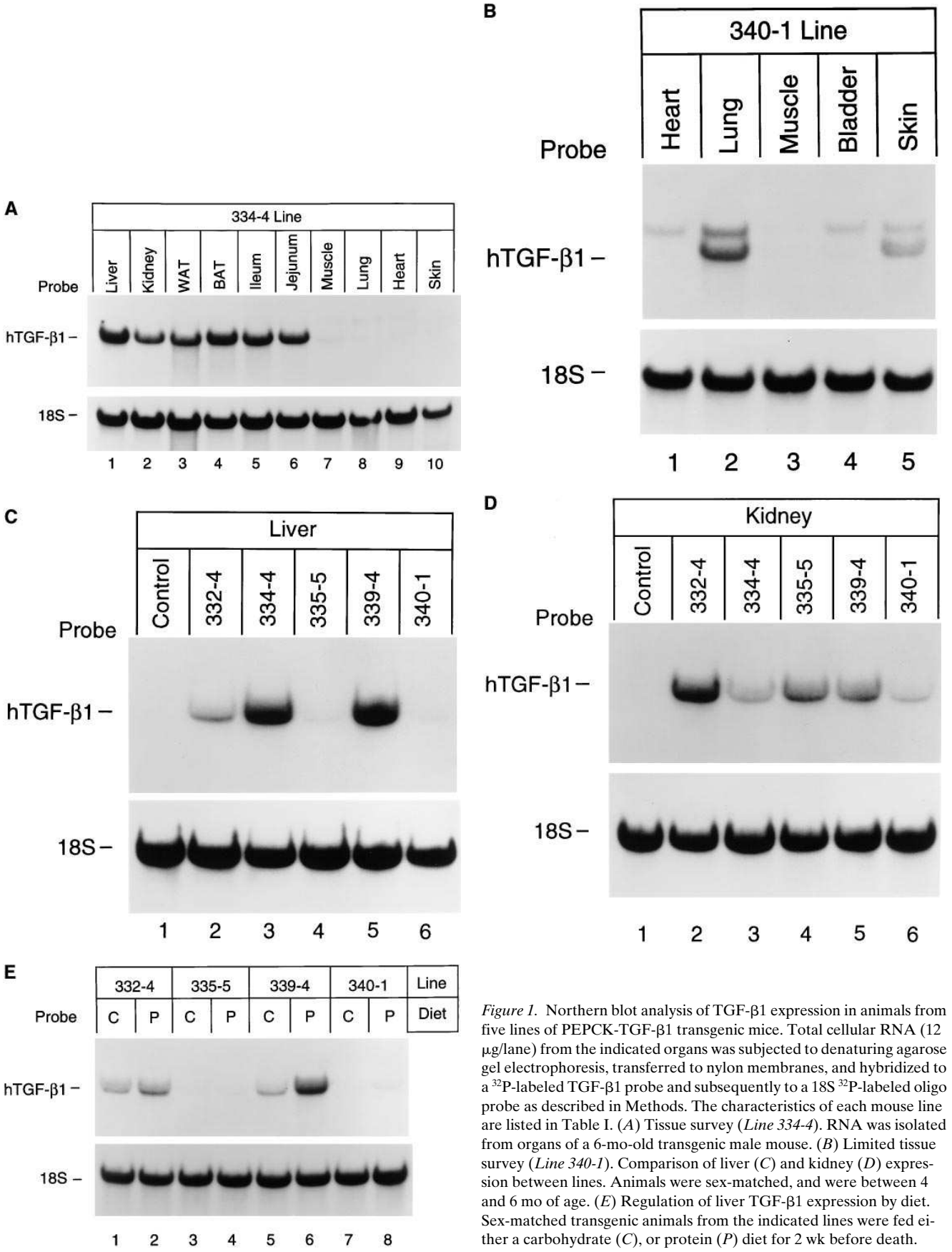


*Figure 1.* Northern blot analysis of TGF-β1 expression in animals from five lines of PEPCK-TGF-β1 transgenic mice. Total cellular RNA (12 μg/lane) from the indicated organs was subjected to denaturing agarose gel electrophoresis, transferred to nylon membranes, and hybridized to a $^{32}$P-labeled TGF-β1 probe and subsequently to a 18S $^{32}$P-labeled oligo probe as described in Methods. The characteristics of each mouse line are listed in Table I. (*A*) Tissue survey (*Line 334-4*). RNA was isolated from organs of a 6-mo-old transgenic male mouse. (*B*) Limited tissue survey (*Line 340-1*). Comparison of liver (*C*) and kidney (*D*) expression between lines. Animals were sex-matched, and were between 4 and 6 mo of age. (*E*) Regulation of liver TGF-β1 expression by diet. Sex-matched transgenic animals from the indicated lines were fed either a carbohydrate (*C*), or protein (*P*) diet for 2 wk before death.

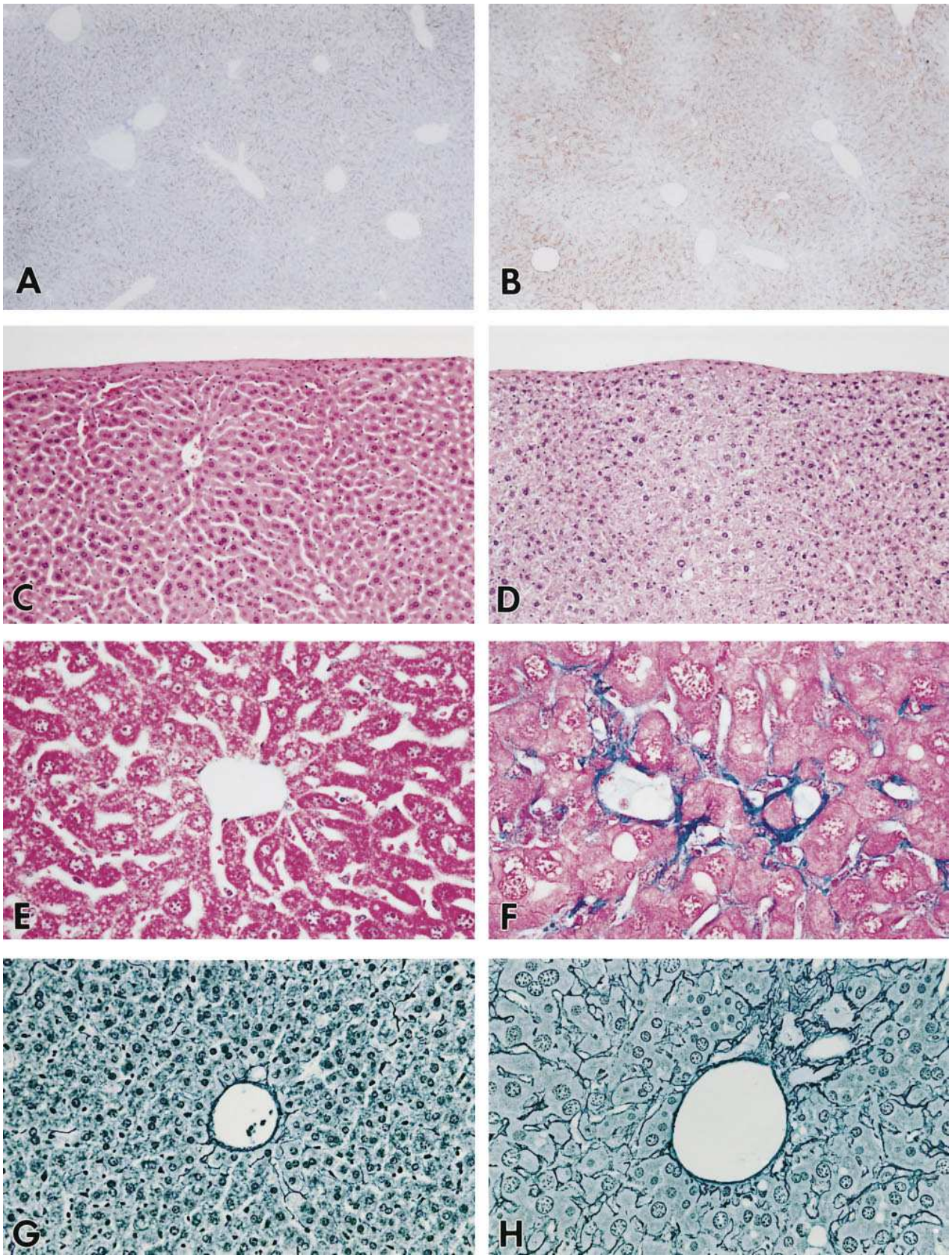


*Figure 2.* Histology of the liver in TGF-β1 transgenic mice. (*A* and *B*) Immunohistochemical localization of TGF-β1. (*A*) In a control animal, TGF-β1 immunoreactivity (*red*) is evenly distributed throughout the liver and is localized to the basolateral surface of hepatocytes (75×). (*B*) In a transgenic animal (line 332-4) TGF-β1 immunoreactivity is most abundant in periportal hepatocytes and falls off toward perivenous areas (75×). (*C* and *D*) Hematoxylin and eosin. (*C*) Normal liver (120×). (*D*) Liver from a 6-mo-old transgenic male of line 332-4 (120×). There is

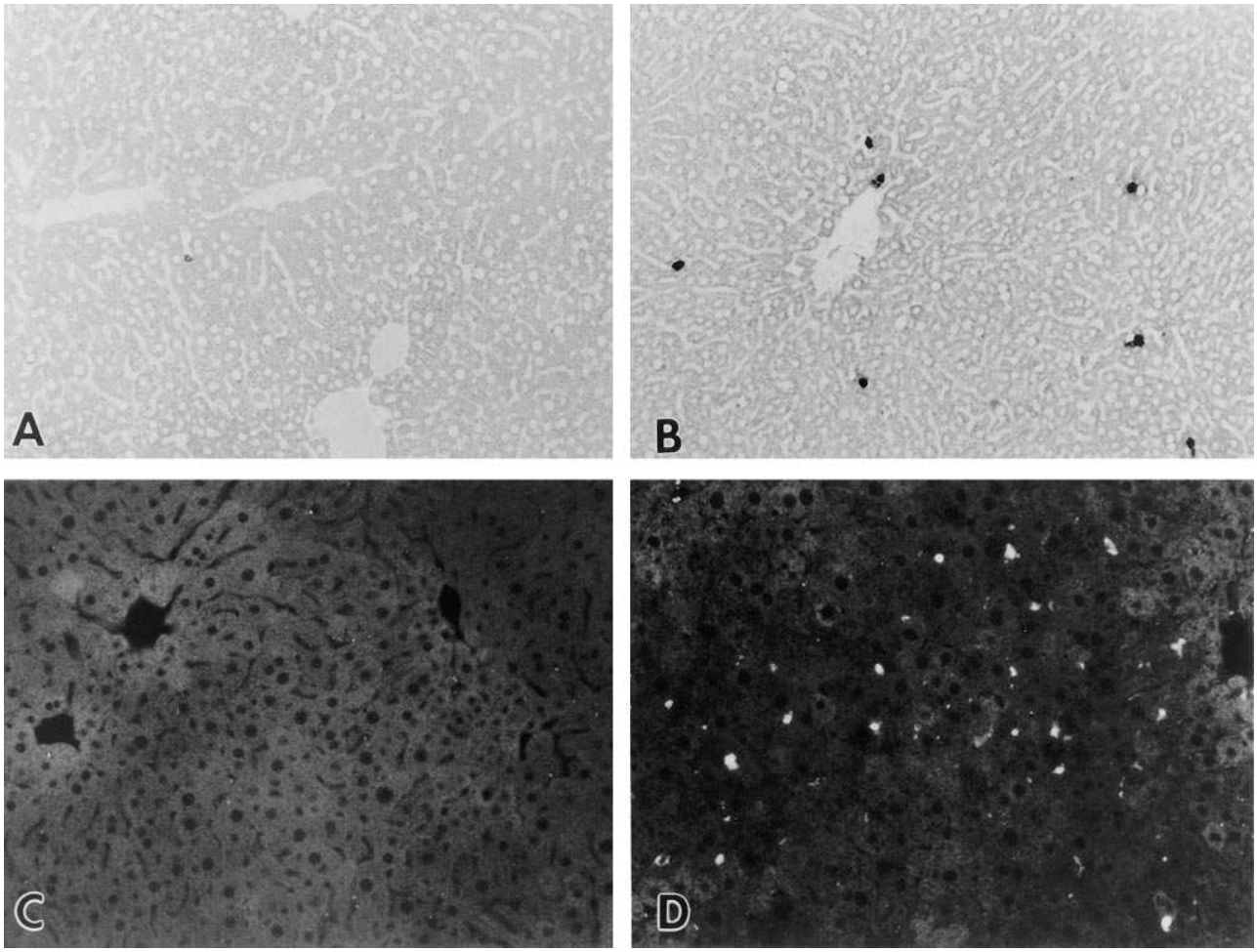


*Figure 3.* Hepatocyte proliferation and death in TGF-β1 transgenic mice. (*A* and *B*) Proliferating hepatocytes were marked by bromodeoxyuridine labeling, and were detected by immunohistochemical methods using DAB as the substrate (described in Methods). Sections were not counterstained. (*A*) Normal liver (144×). (*B*) Liver from a 6-mo-old transgenic male of line 332-4 (144×). (*C* and *D*) Apoptotic cells were detected using the TUNEL assay as described in Methods. (*C)* Normal liver (180×). (*D*) Liver from a 6-mo-old transgenic mouse of line 334-4. There are numerous apoptotic bodies throughout the field (180×).

nucleosomal DNA fragmentation (TUNEL assay) (Fig. 3, *C* and *D*). While control livers showed the occasional TUNEL-positive cell (Fig. 3 *C*), many apoptotic nuclei could be seen in transgenic livers (Fig. 3 *D*). This loss of hepatocytes through apoptosis was clearly sufficient to initiate a compensatory proliferative response as judged by increased hepatocyte BrdU labeling, yet was insufficient to cause any decrease in overall mass. This result indicates that exposure of hepatocytes to high levels of active TGF-β1 can result in significant hepatocyte cell death.

To compare the cell specificity of endogenous TGF-β1 expression with that directed by the rat PEPCK 5′ regulatory sequences in kidney, immunohistochemical analysis was performed on sections of kidney from transgenic and control age- and sex-matched littermates. In control animals, TGF-β1 expression was localized to the proximal convoluted tubule epithelium of the juxtamedullary nephrons (Fig. 4 *A*). Immunoreactive deposits were localized intracellularly, suggesting that this is the site of TGF-β1 synthesis in the normal adult mouse kidney. In transgenic kidneys, TGF-β1 immunoreactivity was also localized to proximal tubule epithelium of juxtamedullary nephrons, and in addition, to proximal tubule epithelium of both midcortical and superficial nephrons (Fig. 4 *B*). This specific regional pattern of expression of the TGF-β1

*Figure 2 legend (Continued)*

marked cellular heterogeneity and an increase in vacuolated hepatocytes. The surface of the liver is uneven, which typifies regenerative growth. (*E* and *F*) Masson's trichrome stain. (*E*) Normal liver (376×). (*F*) Liver of an 8-mo-old transgenic male of line 339-4; there is marked perisinusoidal collagen deposition (*blue*) (376×). (*G* and *H*) Reticulin stain. (*G*) Normal liver (224×). (*H*) Liver from an 8-mo-old transgenic male of line 339-4. There is an increase in hepatocyte size that disrupts the normal hepatic architecture (224×).

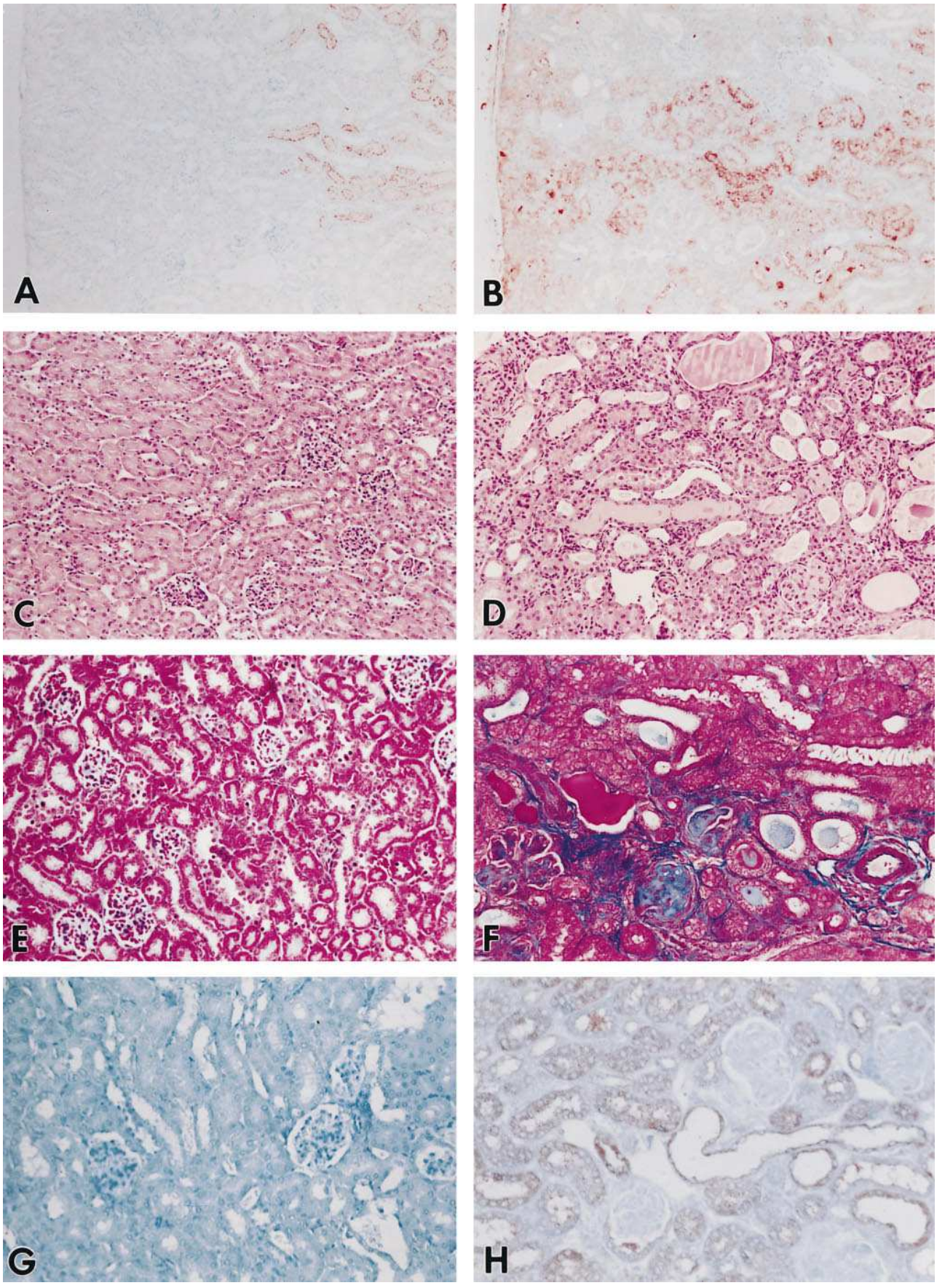
A
B
C
D
E
F
G
H

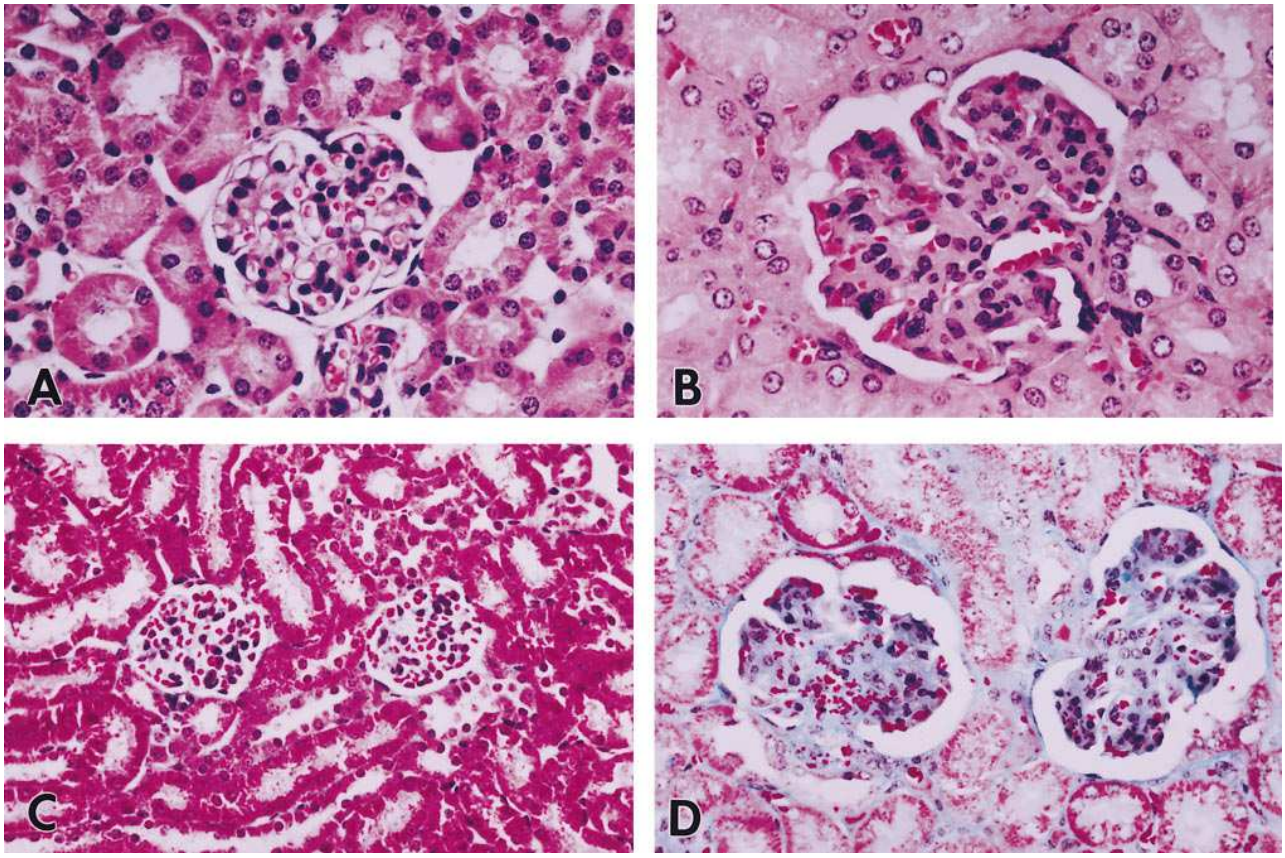


*Figure 5.* Histology of renal glomeruli in TGF-β1 transgenic mice. (*A* and *B*) Hematoxylin and eosin. (*A*) Glomerulus of a control animal. Capillary loops are prominent and well expanded (420×). (*B*) Glomerulus from a 6-mo-old transgenic animal. There is marked thickening of the glomerular tuft and collapse of the capillary loops (420×). (*C* and *D*) Masson's trichrome stain. (*C*) Normal kidney (300×). (D) Glomeruli of an 8-mo-old transgenic male mouse. Note marked collagen deposition (*blue*) within the glomerular tuft and mesangium (300×).

transgene has been reported for endogenous PEPCK expression, and for structural genes whose expression is directed by 5′ PEPCK regulatory sequence (17).

To assess the consequences of chronic overexpression of active TGF-β1 expression in proximal tubule epithelium on renal morphology, kidneys from control and transgenic mice of several lines were removed and processed for light microscopic examination (Fig. 4 *C*). The kidneys of transgenic mice showed dilation of the proximal tubules, flattened atrophic tubular epithelial cells, and protein casts within many tubules. Dilation of some of the distal collecting ducts and segments of the loop of Henle were also evident (data not shown). To assess the regional specificity and magnitude of the fibrotic response to TGF-β1 expression, sections of kidney were processed for assessment of collagen deposition as well as for fibronectin and PAI-1 immunoreactivity. In transgenic kidneys, marked collagen deposition was localized to the renal interstitium surrounding the proximal tubules, and within glomeruli (Fig. 4 *F*). Intense fibronectin immunoreactivity was localized to the renal interstitium (data not shown), and PAI-1 immunoreactivity was localized to the proximal tubule epithelium in both midcortical and superficial nephrons (Fig. 4 *H*).

Glomerular disease was a prominent feature of the renal pathology associated with chronic TGF-β1 expression. There was a marked loss of glomeruli from the juxtamedullary, midcortical, and superficial zones. Many of the remaining nephrons contained enlarged collagen-laden glomeruli with collapsed capillaries, thickened glomerular tufts, and in some cases thickened basement membranes (Fig. 5 *B*). Fibrin was deposited along some afferent arterioles, suggesting that a cellular repair response had occurred. In a few cases, this repair was accompanied by proliferation of juxtaglomerular appara-

*Figure 4.* Histology of the kidney in PEPCK-TGF-β1 transgenic mice. (A and *B*) Immunohistochemical localization of TGF-β1. (*A*) In a control animal, TGF-β1 immunoreactivity (*red*) is localized to the proximal tubule epithelium of juxtamedullary nephrons (90×). (*B*) In a transgenic animal, TGF-β1 immunoreactivity is localized to proximal tubule epithelium of superficial, midcortical, and juxtamedullary nephrons (90×). (*C* and *D*) Hematoxylin and eosin. (*C*) Normal kidney (120×). (*D*) Kidney from a 6-mo-old transgenic male. There is marked tubular epithelial dropout, tubule dilatation, and numerous protein casts (120×). (*E* and *F*) Masson's trichrome stain. (*E*) Normal kidney (180×). (*F*) Kidney from an 8-mo-old transgenic male. Collagen (*blue*) deposition is prominent in the interstitium surrounding the proximal tubules and in glomeruli (165×). (*G* and *H*) Immunolocalization of plasminogen activator-1 (PAI-1). (*G*) Normal kidney (192×). (*H*) Kidney from an 8-mo-old transgenic male. PAI-1 immunoreactivity is prominent and is localized to the epithelium of proximal tubules (211×).

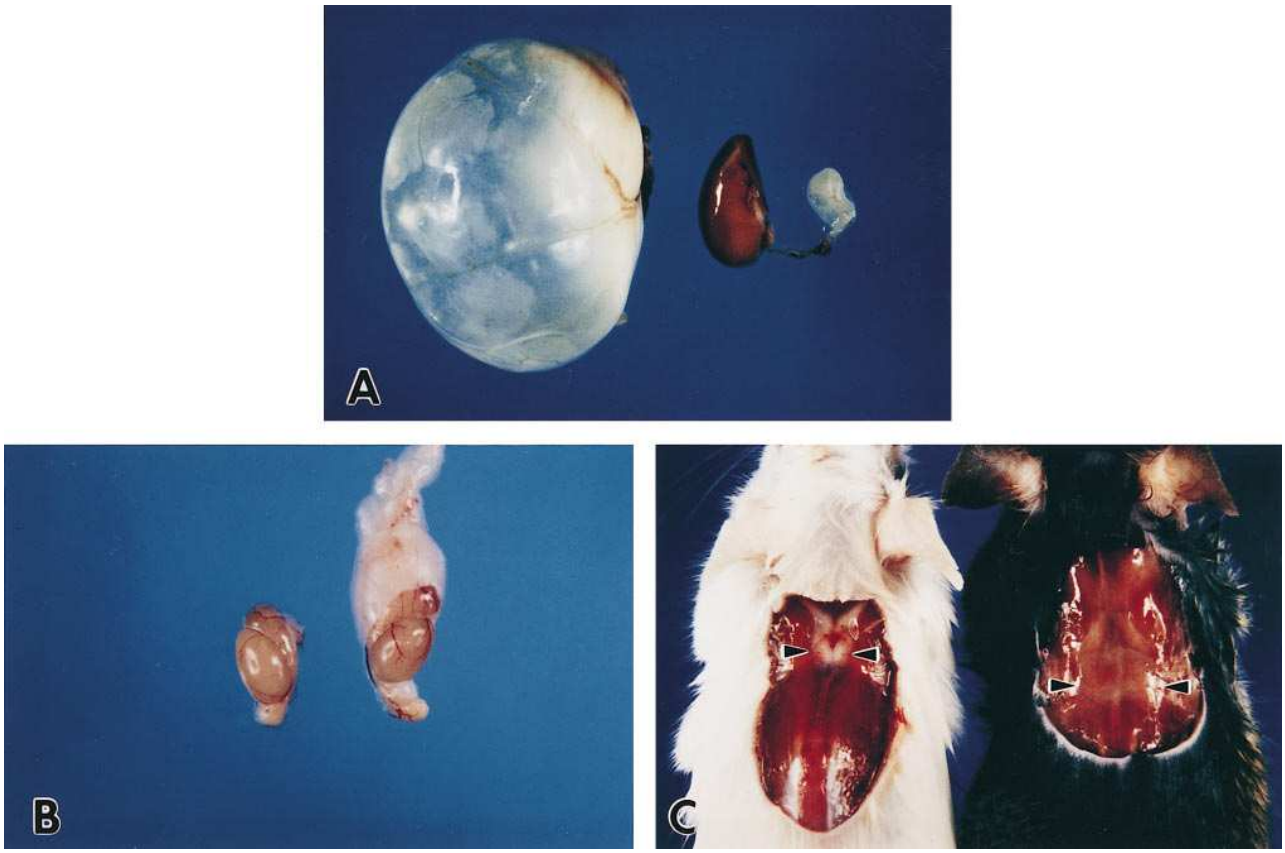


*Figure 6.* Kidney and adipose tissue: gross pathology in line 340-1 transgenic mice. (*A*) Hydronephrotic kidney of a 10-mo-old transgenic male (*left*) compared with a kidney and bladder from a control animal. Only a thin rim of sclerotic cortex remains. (*B*) Testis, epididymis, and gonadal fat pad from an 8-mo-old transgenic (*left*) and age-matched control mouse. (*C*) Interscapular BAT of an 8-mo-old transgenic (*left*) and age-matched control mouse. The boundaries of the BAT are marked by arrowheads. Note the difference in size and marked change in the color of BAT in the transgenic mouse.

tus (data not shown). There was no evidence of widespread fibrotic interruption of the vasculature.

Of the five lines of mice that were established and characterized, mice from two lines (332-4 and 340-1, Table I) exhibited massive unilateral or bilateral fluid-filled kidneys (Fig. 6 *A*). In all cases examined histologically, the affected kidneys were urine-filled sacs consisting of only a thin rim of sclerotic cortex. In some cases the ureters were enlarged and dilated, suggestive of a block in urine flow at a point distal to the renal pelvis. Even after severing the ureter, however, urine was retained within the kidney, suggesting that secondary blocks had occurred within the kidney. While $\sim$ 70% of the animals in these two lines exhibited either gross or histologic evidence of hydronephrosis, only $\sim$ 5% of the transgenic animals exhibited severe hydronephrosis that resulted in death.

Of the 32 founder transgenic animals, 27 exhibited a moderate to severe loss of elasticity of haired skin, making manual restraint difficult. To characterize the underlying cause of this lesion, dorsal trunk skin from control and transgenic mice was removed and examined histologically. The PEPCK regulatory sequences used to target TGF-β1 expression directed expression to both the epidermis and subcutaneous adipose tissue (data not shown), known sites of PEPCK expression (32). While the epidermis appeared unaffected by expression of active TGF-β1, there was both a severe reduction in subcutaneous fat and marked fibrosis (data not shown). It is presumed that the severe fibrosis of the adipose tissue is the underlying cause of the loss of skin elasticity, thus creating a tight-skin phenotype.

Transgenic mice from four of the five lines characterized (Table I) exhibited a dramatic reduction in, and severe fibrosis of all white fat depots, including gonadal, perirenal, omental, inguinal, interscapular, and mammary. The near complete absence of the mammary gland fat pad severely impaired both the pubertal and pregnancy-dependent development of the mammary gland, rendering females completely lactation-deficient (data not shown). The magnitude of the loss of adiposity was influenced by genetic background. The severity of the loss and resulting morbidity increased with successive backcrosses to C57Bl/6. We were unable to obtain viable transgenic mice past the third Bl/6 backcross, as mortality generally occurred during the first few days of postnatal life.

To evaluate the overall extent of the loss of adipose tissue, carcasses including all abdominal and thoracic viscera from control and transgenic male mice (line 340-1) were subjected to proximate analysis. While total body protein, ash, crude fiber, and carbohydrate content was not significantly altered by TGF-β1 expression, total body fat content was reduced by

*Table II. Phenotypic Differences Between Wild-type, TGF-β1 Transgenic, and TGF-β1:ob/ob Transgenic Mice*

| Animal[a] | | | | Organ wt/body wt (%) | | | | |
|---|---|---|---|---|---|---|---|---|
| Group | Genotype | Sex | Body wt | Liver | Spleen | Plasma triglyceride | Plasma cholesterol | Carcass fat[b] |
| | | | *g* | | | *mg/dl* | *mg/dl* | % |
| A | Wild-type | M | 32.0 (1.6) | 5.0 (0.2) | 0.31 (0.05) | 75.7 (16.1) | 110.7 (11.7) | 6.14 (0.91) |
| | | F | 28.1 (1.1) | 4.9 (0.1) | 0.38 (0.02) | 89.0 (6.7) | 85.6 (6.1) | |
| B | TGF-β | M | 26.4 (1.3) | 5.9 (0.2)* | 0.72 (0.09)* | 181.0 (42.3) | 103.8 (11.7) | 2.65 (0.17)§ |
| | | F | 23.2 (1.3) | 5.9 (0.2)‡ | 0.65 (0.05)§ | 162.4 (20.0)* | 92.0 (3.3) | |
| C | *ob/ob* | M/F | 62.2 (2.8) | 5.9 (0.4) | 0.17 (0.02) | ND | ND | ND |
| D | *ob/ob*:TGF-β | M/F | 28.2 (2.0)§ | 14.4 (1.4)§ | 0.87 (0.08)§ | ND | ND | ND |

Values are means (≥ five animals); numbers in parentheses are SEM. Significance was assessed by two-tailed, unpaired Student's *t* test; $*P < 0.05$, $‡P < 0.01$, $§P < 0.005$. [a]Groups A and B: 21-wk-old control and TGF-β1 transgenic mice from line 340-1. Groups C and D: 24-wk-old male and female *ob/ob* and TGF-β1:*ob/ob* transgenic mice from line 340-1. *ob/ob* genotype screening was performed as described in Methods. [b]Carcass fat was assessed by proximate analysis (five mice/group) as described in Methods.

~ 60% (Table II). To assess the onset and determine the precise magnitude of TGF-β1's effects on white fat accretion, we quantified the change in epididymal fat pad mass from control and transgenic mice beginning at day 3 (Fig. 7 *A*). In control hybrid mice, the mean epididymal fat pad mass increased rapidly from 3 to 12 d of age, reaching 145 mg by 130 d of age. In transgenic mice, TGF-β1's effects were evident as early as day 3, where transgenic fat pads were smaller than the pads of control littermates. Although transgenic fat pads continued to increase in weight throughout the period examined, the increase was slight such that by 130 d of age, the mean epididymal fat pad mass from transgenic mice was ~ 14-fold less than from control mice.

Normal accumulation of WAT mass occurs through both adipocyte proliferation and triglyceride accumulation. To determine whether the reduction in WAT stores in transgenic mice was due to a block in adipocyte proliferation, differentiation, or to a failure to accumulate triglycerides, we quantified the changes in perinatal epididymal fat pad cell number by determining the DNA content of the pad (Fig. 7 *B*). In control animals, during the period in which the fat pad increased in size and weight, the cell number per milligram of wet weight of tissue decreased. In transgenic mice, while the fat pads were reduced both in size and weight during this same period, there were more cells per unit mass. This difference in transgenic pad cell number could be due to the inability of preadipocytes to differentiate and store triglyceride, and could also reflect a change in the cellular composition of the pad.

On gross inspection, in addition to the WAT pads from transgenic mice of lines 332-4 and 340-1 being dramatically smaller than control fat pads, they were extremely firm and had lost all elasticity (Fig. 6 *B*). This difference was evident in both epididymal and inguinal fat pads as early as day 5 postpartum. On histologic examination, epididymal fat pads from control mice consisted of unilocular adipocytes of uniform size separated by small amounts of connective tissue (Fig. 8 *A*). In contrast, fat pads from 8-mo-old transgenic mice consisted of a very small collection of unilocular adipocytes separated by the dense accumulation of stromal cells and extracellular matrix (Fig. 8 *B*). Thus, expression of TGF-β1 in developing WAT stores caused a dramatic change in the cellular composition of the pad.

The increased cellularity of the transgenic fat pad, in combination with the reduction in size and altered cellular composition, suggested that TGF-β1's effects on WAT accumulation occur by inhibiting adipocyte differentiation. To assess TGF-β1's effects on WAT differentiation, epididymal fat pads from control and transgenic mice (line 340-1) were isolated on days 16, 26, and 35, and total cellular RNA was probed for expression of specific markers of adipocyte differentiation (Fig. 9). TGF-β1 was expressed in WAT as early as day 5 postpartum (data not shown), with expression remaining constant throughout the period examined. The expression of all three markers of adipocyte differentiation examined—lipoprotein lipase (LPL), C/EBP-α and endogenous PEPCK—were greatly reduced in transgenic WAT at all time periods. This result indicates that expression of TGF-β1 in developing adipose tissue inhibits the terminal differentiation of the majority of adipocytes. Presumably, use of the PEPCK regulatory sequences to direct transgenic expression permitted an initial wave of adipogenesis to occur before the transgene was transcriptionally activated and TGF-β1 exerted its effects. While the expression of adipocyte-specific markers was clearly reduced in the WAT of transgenic mice, the magnitude of the reduction is probably overestimated due to the marked fibroplasia, and thus altered cellular composition of the pad.

All four lines of mice that exhibited the severe reduction in WAT and associated fibrosis displayed similar alterations in BAT. Normal interscapular BAT is veiled by a thin layer of WAT, is amber in color, and is dense, but pliable. In contrast, BAT lobes from transgenic mice were easily discernible due to the absence of WAT, and were white and extremely firm and rigid (Fig. 6 *C*). This gross change was evident as early as day 1 postpartum. Similar to transgenic WAT, BAT pads from transgenic mice were smaller than controls at all ages examined (Fig. 7 *C*). The reduction in size was accompanied by a dramatic change in morphology. Normal brown fat consists of polygonal, multilocular adipocytes that are surrounded by capillaries and reticular fibers (Fig. 8 *C*). In transgenic mice, most of the brown adipocytes were unilocular, and the intervening connective tissue separating cells and lobules was massively thickened. In most animals from line 332-4, there were also distinct foci of chondrocytic metaplasia within interlobular septa (Fig. 8 *D*).

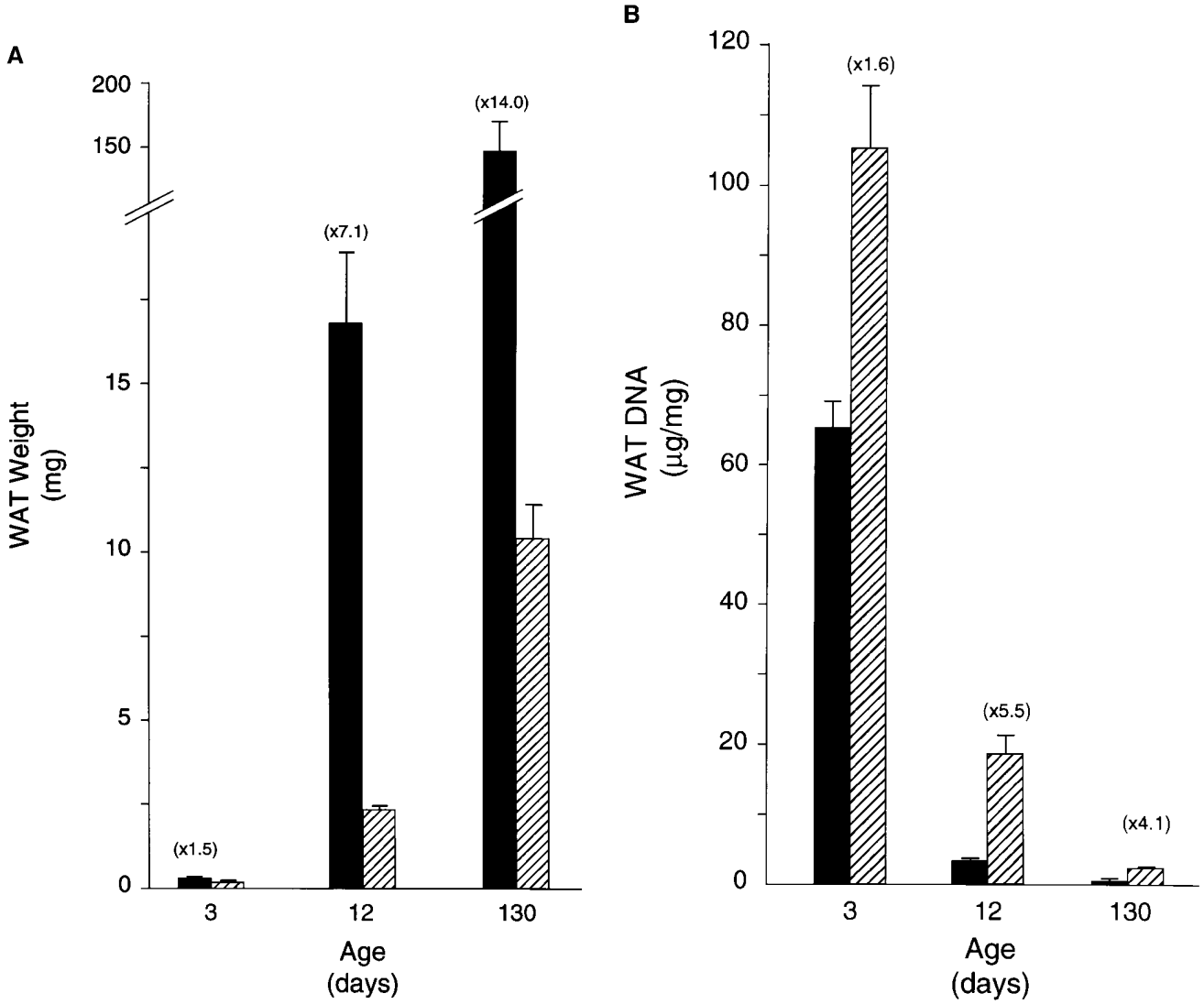


*Figure 7.* Characterization of changes in adipose tissue mass in transgenic mice of the 340-1 line. Values are means±standard errors with a minimum of three animals at each time point. Control animals (*solid bars*); transgenic animals (*hatched bars)*. Numbers in parentheses indicate fold difference between control and transgenic values for each time point. (*A*) Epididymal fat pads were isolated by microdissection from mice at the indicated times, combined and weighed. (*B*) The DNA content of epididymal fat pads isolated in *A* was determined as described in Methods. In controls, one fat pad per animal was used; in transgenics, both pads were combined and used for DNA quantitation. (*C*) Interscapular brown fat pads were isolated at the indicated times and weighed.

The physiologic consequences of a near absence of WAT was assessed macroscopically by determining the changes in the size of abdominal organs and by quantifying the plasma levels of cholesterol and triglycerides. In 6-mo-old transgenic animals from line 340-1, there was a modest increase in the liver-to-body weight ratio and an approximately twofold increase in the spleen-to-body weight ratio in both males and females (Table II). Increased liver size was associated with a mild degree of microvesicular lipid accumulation within hepatocytes (data not shown). There was a modest increase in plasma triglycerides in transgenic mice, while plasma cholesterol was normal. The severe absence of fat stores in viable transgenic mice allowed us to address the pathophysiologic consequences of removing/ablating fat depots from genetically obese mice. To perform these experiments, we placed the TGF-β1 locus from line 340-1 into the *ob/ob* background. As expected, expression of active TGF-β1 in *ob/ob* mice prevented the enormous fat accumulation which typifies the phenotypic consequences of this genetic defect. As a consequence of this inability to expand adipose tissue mass, TGF-β:*ob/ob* mice developed massive hepatomegaly and splenomegaly (Table II). The dramatic increase in the liver/body weight ratio was due almost exclusively to both micro- and macrovesicular accumulation of lipids within hepatocytes (data not shown).

## Discussion

We have demonstrated that ectopic overexpression of active TGF-β1 directed by the PEPCK regulatory sequences induces pathologic matrix accumulation in the liver, kidney, and adipose tissue, resulting in severe fibrotic disease. Expression of TGF-β1 in liver resulted in altered hepatocyte turnover and a

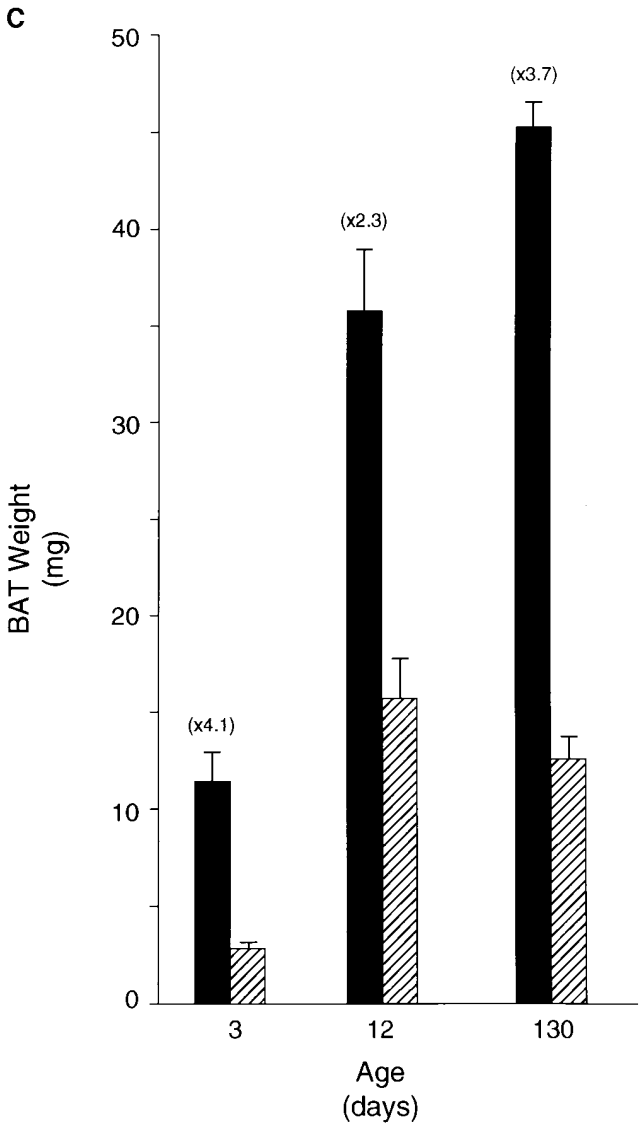


*Figure 7 (Continued)*

modest disruption of liver function. Early mortality was observed in 11% of founder mice as a consequence of hepatic hemorrhage and thrombosis. Renal disease was characterized by excessive deposition of ECM components that caused tubulointerstitial fibrosis and glomerulosclerosis. Severe obstructive uropathy occurred with low penetrance. Expression of TGF-β1 in differentiating adipocytes blocked normal adipose accretion. The failure of fat to accumulate was due to a TGF-β1–induced block in adipocyte differentiation.

The most common and striking consequence of TGF-β1 expression was the extreme interstitial deposition of extracellular matrix in organs in which the transgene was expressed. Aberrant expression of TGF-β1 is now firmly held as a primary determining factor in the development of fibrotic diseases such as glomerulonephritis, arthritis, and cirrhosis (7), all of which are characterized by increased extracellular matrix accumulation. These conditions commonly develop in response to chronic injury or inflammation, where, in an attempt to continually repair cellular damage and maintain tissue architecture, the normal wound healing response fails to be curtailed.

In normal and damaged liver, matrix production has been ascribed to the lipocyte, or fat-storing cell (33). In normal liver, these cells possess low mitotic activity and are primarily involved in the storage of vitamin A within large triacylglycerol-rich droplets. In response to injury, however, lipocytes become activated, a process that includes enhanced proliferation and transformation to a myofibroblast-like cell type. Lipocytes are activated by TGF-β1, express TGF-β receptors, and synthesize and secrete latent TGF-β1 (34). Vascular endothelial cells can activate latent TGF-β1, demonstrating that both autocrine and paracrine loops are involved in TGF-β1–induced lipocyte activation (35). In PEPCK-TGF-β1 mice, we have bypassed the requirement for activation of latent TGF-β1 by overexpressing a constitutively active form of the molecule in hepatocytes. This elevated local pool of active TGF-β1 presumably maintains lipocytes in an active state, resulting in excessive ECM production and development of hepatic fibrosis.

A role for TGF-β1 in coordinately regulating liver homeostasis during normal, regenerating, and hyperplastic liver growth has been suggested. This theory is based in part on the increased expression of TGF-β1 during periods of hepatic growth, and on TGF-β1's potent antiproliferative effects on hepatocytes in culture (8). In addition, TGF-β1 can induce hepatocyte cell death both in vitro and in vivo (36). Despite these compelling data, definitive in vivo evidence of TGF-β1's precise role in maintaining liver homeostasis is lacking. It is clear from our results and those of Sanderson et al. (37) that exposing developing or mature hepatocytes to active TGF-β1 induces hepatocyte cell death. The incidence of hepatocyte apoptosis induced by TGF-β1 is relatively small, however, even minimal increases can be of considerable biological importance (38). This moderate increase in hepatocyte cell death was nevertheless sufficient to initiate a compensatory increase in hepatocyte proliferation, resulting in maintenance of near normal liver mass. Whether TGF-β1 induces hepatocyte cell death by direct stimulation of the cell death machinery, or indirectly through induction of fibrosis that can terminally damage hepatocytes (39), is unknown.

If TGF-β1 is a regulator of liver homeostasis, then based on our transgenic results and those of Sanderson et al. (37), along with the absence of any perturbation in hepatic homeostasis in TGF-β null mice (40, 41), it appears that TGF-β1 signaling is not required, or has only a minimal function in quiescent liver. It is more likely that signaling is necessary to regulate liver growth during conditions in which liver homeostasis is perturbed. This possibility is supported by data showing that TGF-β1 can negatively influence hepatocyte proliferation at certain periods during regeneration after 70% partial hepatectomy (42, 43). Further studies, however, are required to investigate specific pathways involved in TGF-β1's control of the hepatocyte cell cycle, both during regenerative and hyperplastic liver growth. The PEPCK- and albumin–TGF-β1 transgenic mice should therefore be of use in clarifying TGF-β1's role in the regulation of hepatic mass.

Three distinct kidney pathologies: glomerulonephritis, tubulointerstitial fibrosis and injury, and hydronephrosis, were evident in PEPCK-TGF-β1 transgenic mice. Thickening of the glomerular tuft, capillary loop collapse, and matrix accumulation were the most prominent glomerular changes, while interstitial damage was characterized by intratubular cast formation, tubular atrophy, and marked interstitial fibrosis. The glomerular changes were apparent in all lines of transgenic mice ana-

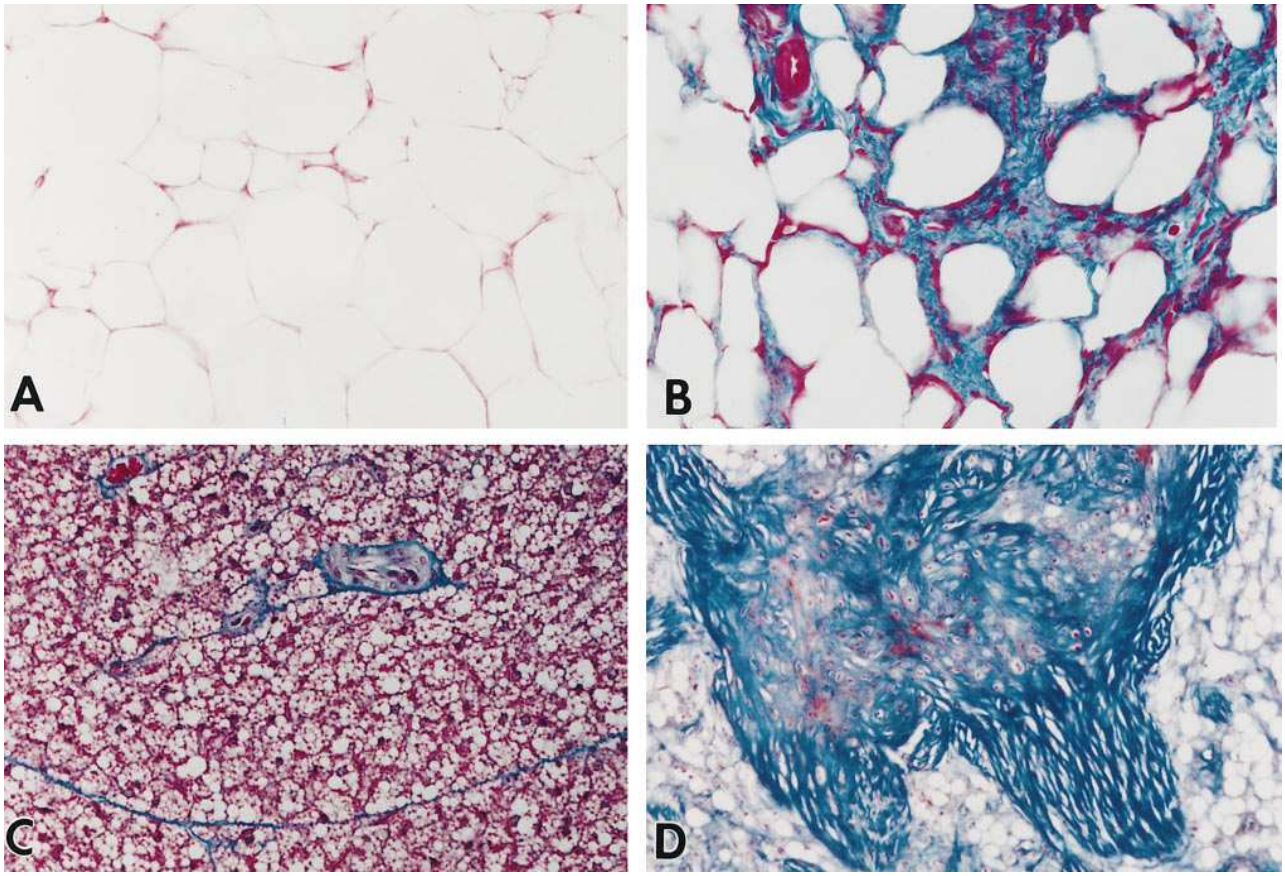


*Figure 8.* Histology of WAT and BAT in line 340-1 transgenic mice. Masson's trichrome stain. (*A* and *B*) Epididymal fat. (*A*) Control animal (280×). (*B*) Transgenic 8-mo-old animal (280×). There is a marked accumulation of extracellular collagen (320×). (*C* and *D*) Interscapular brown fat. (*C*) Control animal. The lobules are divided by thin septa (*blue*) and the adipocytes are multilocular (214×). (*D*) Transgenic 8-mo-old animal. There is marked extracellular collagen deposition, chondrocytic metaplasia, and adipocytes are unilocular (214×).

lyzed. PEPCK is not expressed in glomeruli, and PEPCK-directed transgenes, including the human TGF-β1 cDNA, are not targeted to glomeruli (17, 31). Therefore, the glomerulosclerosis observed in PEPCK-TGF-β1 mice occurs either as a consequence of tubular changes and interstitial fibrosis, or is due most likely to circulating active TGF-β1. The latter hypothesis is supported by the observations that transgenic mice that express active TGF-β1 exclusively in hepatocytes develop glomerular lesions (44) that are remarkably similar to those found in the PEPCK-TGF-β1 mice.

Enhanced ECM accumulation was evident in both glomeruli and in the tubule interstitium. The increased tubule and interstitial matrix deposition may be due, at least in part, to TGF-β1–induced alterations in fibrinolysis and enhanced synthesis of matrix components. Both PAI-1 and fibronectin immunoreactivity were markedly elevated within and immediately surrounding, the tubule epithelium. Excessive renal matrix accumulation has been specifically linked to inhibition of the plasmin protease system through elevated PAI-1 expression, at least within glomeruli (45, 46). In this study, we demonstrate that expression of TGF-β1 within proximal tubular epithelial cells upregulates PAI-1 expression, specifically within this compartment. The importance and relative contribution of tubular epithelial expression of active TGF-β1 to the development of tubular lesions and interstitial fibrosis, however, is uncertain. Tubulointerstitial damage is also associated with chronic kidney disease irrespective of the compartment from which the disease originates (47). This fact, however, can be addressed by determining the onset of the tubular and interstitial lesions relative to the timing of glomerular changes. If the tubular lesions occur before glomerular changes, this would indicate that these changes may be a direct consequence of active TGF-β1 expression from this site.

Development of severe hydronephrosis was not a highly penetrant phenotype in PEPCK-TGF-β1 mice. Early signs of hydronephrosis, however, were seen in the majority of animals from lines 332-4 and 340-1 whose kidneys were examined histologically. This observation was characterized by progressive disappearance of regions of the medulla from 30 d of age. Potential causes of hydronephrosis are many and diverse. One cause is the formation of renal stones due to tubular dysfunction, which can result in a blockage at different points along the urinary tract (48). To further complicate dissection of the effects of transgene expression on the different renal compartments, tubular changes have also been observed in an animal model of experimental hydronephrosis induced by unilateral ureteral ligation. In this case, increased TGF-β1 expression was observed during the early stages of hydronephrosis, and

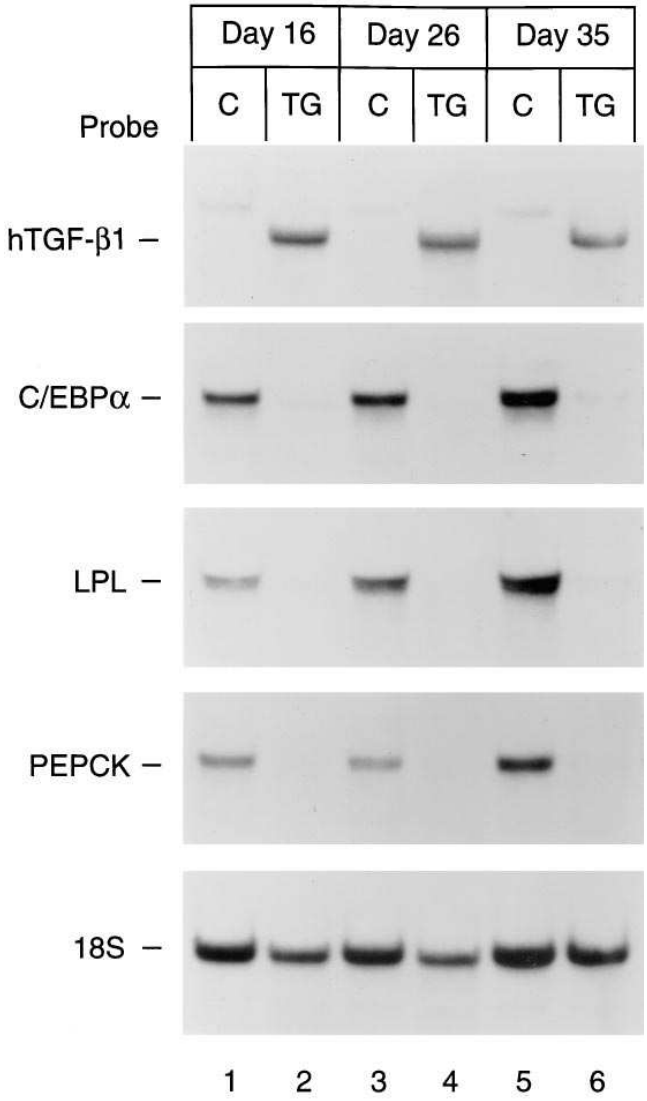


*Figure 9.* Molecular characterization of WAT differentiation in line 340-1 transgenic mice. Total cellular RNA was extracted from microdissected epididymal fat pads of control (*C*) and transgenic (*TG*) mice at the indicated times and subjected to Northern analysis. The filter was hybridized with a $^{32}$P-labeled human TGF-β1 probe and subsequently stripped and hybridized with a succession of probes for stage-specific markers of adipocyte differentiation. These included C/EBP-α, LPL, and PEPCK. Equality of RNA loads was assessed by hybridization with a $^{32}$P-labeled 18S oligonucleotide probe.

was believed to be the cause of proximal tubular apoptosis observed during the later stages (49). TGF-β1 may therefore be capable of exerting proapoptotic effects on tubules that could contribute to the development of hydronephrosis.

The possibility that the TGF-β1 transgene was expressed at other sites within the urinary tract, resulting in fibrosis and restriction urinary flow, was also investigated. In bladder, both the transitional epithelia of the mucosa and the smooth muscle cells of the muscularis are sites of PEPCK expression (31). Bladder from line 340-1 expressed the transgene, albeit at a low level, and was fibrotic (data not shown). Thus, expression of active TGF-β1 within the bladder could diminish normal elasticity, at least in some instances leading to impaired urinary output. It is also likely that TGF-β1 produced by the proximal tubule epithelium is secreted into the tubule lumen, and could thereby directly affect the rest of the urinary outflow tract. This exposure could result in fibrosis and loss of urinary output, contributing to hydronephrosis.

The feasibility of alleviating renal fibrosis through blocking TGF-β1's effects on pathological matrix accumulation has been amply demonstrated by the administration of molecules with TGF-β–neutralizing activity such as decorin, TGF-β neutralizing antibodies (50, 51), or antisense oligonucleotides delivered directly to the kidney by gene-transfer technology (52). Other potential therapeutic interventions for control of fibrotic kidney disease involve inhibition of the renin–angiotensin system, as considerable evidence has recently pointed to a link among TGF-β, fibrosis, and this system (53). In glomerulosclerosis, the fibrotic response can be prevented either by angiotensin-converting enzyme inhibitors or by neutralizing antibodies to TGF-β (54, 55). These animals should therefore be a useful tool to investigate further the effectiveness of these and new therapeutic regimes based on amelioration of the fibrotic phenotype.

The most prominent phenotype in PEPCK-TGF-β1 transgenic mice was the extreme paucity of adipose tissue. All fat depots examined were either severely reduced in mass or completely absent, and residual tissue was extremely fibrotic. The reduction in WAT first became apparent during the first few days after birth, suggesting that expression of active TGF-β1 was perturbing adipogenesis.

As PEPCK is a late marker of adipogenesis and is expressed only in terminally differentiated adipocytes (56), it was surprising that expression of TGF-β1 from this regulatory sequence blocked adipose development and accretion. We hypothesize that at least one wave of adipocyte proliferation and differentiation occurred before the transgene was expressed, after which time expression of the transgene inhibited any further adipose development via a negative autocrine loop. The combined analysis of WAT DNA content, S-phase (BrdU) labeling (data not shown), and stage-specific markers of adipogenesis, supports this hypothesis, showing that the majority of transgenic preadipocytes failed to proliferate and/or differentiate.

Until recently, the molecular events associated with adipocyte differentiation were poorly understood. However, the availability of preadipocyte cell lines that undergo terminal differentiation, along with studies on developing adipose tissue, has allowed the elucidation of distinct stages of the differentiation program and identification of molecules that play key roles in this process (for review see references 56, 57, and 58). Studies using cell lines and primary cultures of adipocyte precursor cells isolated from different species have shown that exogenous TGF-β1 is a potent inhibitor of differentiation (12, 13, 16, 59, 60). TGF-β1 appears to be most effective at blocking adipocyte differentiation if added before the expression of the fully differentiated phenotype, is reversible, involves the synthesis of one or more new proteins, and is independent of its effects on cell cycle. The precise stage and the mechanisms by which TGF-β1 inhibits this process, however, are unknown.

TGF-β1 may inhibit adipogenesis directly by modulating the expression of critically required molecules, or indirectly by enhancing ECM synthesis and deposition. A direct effect is not without precedence as TGF-β inhibits myoblast differentiation in vitro by blocking the expression and function of two criti-

cally required muscle-specific transcription factors, MyoD (61) and myogenin (62). While TGF-β1 may directly affect adipogenesis, however, the magnitude of these effects is also likely to be influenced by extracellular matrix. The pericellular environment is often instructive for proliferation and differentiation, and adipocyte differentiation appears to be highly dependent upon downregulation of ECM components, particularly fibronectin (16, 63). The failure of adipose tissue to accumulate in transgenic animals could therefore be due in part to the extreme fibrosis. Thus, direct and indirect mechanisms may account for TGF-β1's modulation of adipocyte differentiation. A definitive assessment of TGF-β1's effects on adipogenesis will require analysis of the expression of ECM components and very early adipocyte-specific markers in perinatal fat pads.

While WAT depots in transgenic mice were severely reduced, interscapular BAT was reduced only by 50%. The extent of this reduction, however, is likely to be underestimated, due principally to the extensive expansion of intervening connective tissue. Both BAT itself and the thin veil of WAT covering it, were the most fibrotic tissues in these mice. This reduction in BAT and extreme fibrosis were both apparent at birth, suggesting that TGF-β1 was influencing the earliest stages of BAT differentiation (data not shown). Northern analysis of control and transgenic BAT also showed decreased expression of the BAT-specific uncoupling protein (UCP or thermogenin). The extent of this decrease, however, was again difficult to quantitate because of the extreme fibrotic nature of the tissue. It thus appears that expression of active TGF-β1 inhibits both WAT and BAT differentiation programs, although perhaps to different degrees. Interestingly, the morphology of residual transgenic BAT was altered from the normal multilocular adipocyte to a larger more unilocular cell. A similar change was also observed in mice overexpressing an $aP_2$-glycerol-3-phosphate-dehydrogenase (GPDH) transgene (64), and is likely attributable to alterations in the accumulation of lipid in BAT. It will be of interest to assess the precise stage at which TGF-β1 exerts its effects on BAT during development.

A family of rare conditions known collectively as the lipodystrophies occurs in humans, and is characterized by a generalized or partial loss of body fat (65). It is not clear whether the defect is intrinsic to the adipocyte, or occurs as a result of paracrine or endocrine action on the adipocyte. Almost all forms of the disease are accompanied by other abnormalities including fatty liver, severe hypertrophy, and cardiomegaly. Metabolic and endocrine abnormalities include either mild or severe insulin resistance, hypertriglyceridemia, and a hypermetabolic state. Although LPL is low, the major cause of the hypertriglyceridemia is overproduction of VLDL in the liver. While not invoking a specific association between aberrant TGF-β1 expression and lipodystrophy, there are similarities between the transgenic mice and some of the clinical sequelae associated with lipodystrophy. Lines of mice with the most severe reduction in WAT exhibited hepatomegaly due primarily to abnormal hepatocyte lipid accumulation, and had mildly elevated plasma triglycerides. The magnitude of the hepatomegaly was more pronounced when animals were fed a high-fat (42%) diet (data not shown), and became severe when the transgene was placed onto the *ob/ob* background. We presume this severe hepatomegaly in transgenic mutant mice is a consequence of hyperphagia and the failure to store triglycerides in fat. Both the fat-deficient PEPCK-TGF-β1 mice and the transgenic *ob/ob* mice will be of interest for further investigation into the metabolic and endocrine abnormalities associated with a nearly complete absence of adipose tissue.

These animals constitute a useful model to address the therapeutic potential of TGF-β antagonists in the amelioration of fibrotic disease, and to investigate the molecular and cellular basis of TGF-β's inhibition of adipocyte differentiation. They will also be of use in determining the precise role of TGF-β1 in liver homeostasis through its regulation of matrix production and hepatocyte proliferation and death in the context of different hepatic challenges.

## Acknowledgments

We thank Dr. Jim Richardson for help with histology and Scott Clark for performing serum triglyceride and cholesterol analyses. We thank Mario Villareal for expert animal care, and Royce Potter for help in preparing this manuscript.

Financial support for this work was provided by National Institutes of Health grants AI28332-01 (D.E. Clouthier), DK09376-01 (S.A. Comerford), and The Perot Family Fund.

## References

1. Kingsley, D.M. 1994. The TGF-β superfamily: new members, new receptors, and new genetic tests of function in different organisms. *Genes Dev.* 8: 133–146.

2. ten Dijke, P., K. Miyazono, and C.H. Heldin. 1996. Signaling via heteroligomeric complexes of type I and type II serine/threonine kinase receptors. *Curr. Opin. Cell Biol.* 8:139–145.

3. Massague, J. 1996. TGF-β signaling: receptors, transducers and mad proteins. *Cell.* 85:947–950.

4. Wrana, J.L., and L. Attisano. 1996. MAD-related proteins in TGF-β signaling. *Trends Genet.* 12:493–496.

5. Roberts, A.B., and M.B. Sporn. 1987. Transforming growth factor-β: potential common mechanisms mediating its effects on embryogenesis, inflammation-repair, and carcinogenesis. *Int. J. Radiat. Appl. Instrum.* 14:435–439.

6. Border, W.A., and N.A. Noble. 1994. Transforming growth factor β in tissue fibrosis. *N. Engl. J. Med.* 331:1286–1292.

7. Border, W.A., and E. Ruoslahti. 1992. Transforming growth factor β in disease: the dark side of tissue repair. *J. Clin. Invest.* 90:1–7.

8. Fausto, N., J.E. Mead, P.A. Gruppuso, A. Castilla, and S.B. Jakowlew. 1991. Effects of TGF-β in the liver: cell proliferation and fibrogenesis. *Ciba Found. Symp.* 157:165–174.

9. Border, W.A., and N.A. Noble. 1994. Transforming growth factor-β in glomerular injury. *Exp. Nephrol.* 2:13–17.

10. Massague, J., and K. Polyak. 1995. Mammalian antiproliferative signals and their targets. *Curr. Opin. Genet. Dev.* 5:91–96.

11. Massague, J., S. Cheifetz, T. Endo, and B. Nadal-Girard. 1986. Type β transforming growth factor is an inhibitor of myogenic differentiation. *Proc. Natl. Acad. Sci. USA.* 83:8206–8210.

12. Ignotz, R.A., and J. Massague. 1985. Type β transforming growth factor controls the adipogenic differentiation of 3T3 fibroblasts. *Proc. Natl. Acad. Sci. USA.* 82:8530–8534.

13. Sparks, R.L., and R.E. Scott. 1986. Transforming growth factor type β is a specific inhibitor of 3T3 T mesenchymal stem cell differentiation. *Exp. Cell Res.* 165:345–352.

14. Heino, J., and J. Massague. 1990. Cell adhesion to collagen and decreased myogenic gene expression implicated in the control of myogenesis by transforming growth factor β. *J. Biol. Chem.* 265:10181–10184.

15. Streuli, C.H., N. Bailey, and M.J. Bissell. 1991. Control of mammary epithelial differentiation: basement membrane induces tissue-specific gene expression in the absence of cell-cell interaction and morphological polarity. *J. Cell Biol.* 115:138–395.

16. Bortell, R., T.A. Owen, R. Ignotz, G.S. Stein, and J.L. Stein. 1994. TGF-β prevents the down regulation of type I procollagen, fibronectin and TGF-β1 gene expression associated with 3T3 L1 preadipocyte differentiation. *J. Cell Biochem.* 54:256–263.

17. Short, M.K., D.E. Clouthier, I.M. Schaefer, R.E. Hammer, M.A. Magnuson, and E.G. Beale. 1992. Tissue-specific, developmental, hormonal, and dietary regulation of rat phosphoenolpyruvate carboxykinase-human growth hormone fusion genes in transgenic mice. *Mol. Cell. Biol.* 12:1007–1020.

18. Hemsley, A., N. Arnheim, M.D. Toney, G. Cortopassi, and D.J. Galas. 1989. A simple method for site-directed mutagenesis using the polymerase chain reaction. *Nucleic Acids Res.* 17:6545–6551.

19. Ikeda, T., M.N. Lioubin, and H. Marquardt. 1987. Human transforming

growth factor type β2: production by a prostatic adenocarcinoma cell line, purification, and initial characterization. *Biochemistry*. 26:2406–2410.

20. Ellis, L., E. Clauser, D.O. Morgan, M. Edery, R.A. Roth, and W.J. Rutter. 1986. Replacement of insulin receptor tyrosine residues 1162 and 1163 compromises insulin-stimulated kinase activity and uptake of 2 deoxyglucose. *Cell.* 45:721–732.

21. Zhang, Y., R. Proenca, M. Maffei, M. Barone, L. Leopold, and J.M. Friedman. 1994. Positional cloning of the mouse obese gene and its human homologue. *Nature*. 372:425–432.

22. Chirgwin, J.M., A.E. Pryzbyla, R.J. MacDonald, and W.J. Rutter. 1979. Isolation of biologically active ribonucleic acid from sources enriched in ribonuclease. *Biochemistry.* 18:5294–5299.

23. Taurog, J.D., S.D. Maika, W.A. Simmons, M. Breban, and R.E. Hammer. 1993. Susceptibility to inflammatory disease in HLA-B27 transgenic rat lines correlates with the level of B27 expression. *J. Immunol.* 150:4168–4178.

24. Bradbury, P., and K.C. Gordon. 1990. Connective tissue and stains. *In* Theory and Practice of Histological Techniques. J.D. Bancroft and A. Stevens, editors. Churchill Livingstone, New York. 119–142.

25. Gavrieli, Y., Y. Sherman, and S.A. Ben-Sasson. 1992. Identification of programmed cell death in situ via specific labeling of nuclear DNA fragmentation. *J. Cell Biol.* 119:493–501.

26. Labarca, C., and K. Paigen. 1980. A simple, rapid, and sensitive DNA assay procedure. *Anal. Biochem.* 102:344–352.

27. Jirtle, R., and S.A. Meyer. 1991. Liver tumor promotion: effect of phenobarbital on EGF and protein kinase C signal transduction and transforming growth factor-β1 expression. *Dig. Dis. Sci.* 36:659–668.

28. Bartels, H., H. Herbort, and K. Jungermann. 1990. Predominant periportal expression of the phosphoenolpyruvate carboxykinase and tyrosine aminotransferase genes in rat liver. *Histochemistry.* 95:637–644.

29. Adachi, M., S. Suematsu, T. Londo, J. Ogasawara, T. Tanaka, N. Yoshida, and S. Nagata. 1995. Targeted mutation in the *Fas* gene causes hyperplasia in peripheral lymphoid organs and liver. *Nat. Genet*. 11:294–300.

30. Wu, H., M. Wade, L. Krall, J. Grisham, Y. Xiong, and T. Van Dyke. 1996. Targeted in vivo expression of the cyclin-dependent kinase inhibitor p21 halts hepatocyte cell-cycle progression, postnatal liver development, and regeneration. *Genes Dev.* 10:245–260.

31. Stolz, A., and N. Kaplowitz. 1990. Biochemical tests for liver disease. *In* Hepatology: A Textbook of Liver Disease. D. Zakim and T.D. Boyer, editors. W.B. Saunders Co., Philadelphia. 637–667.

32. Zimmer, D.B., and M.A. Magnuson. 1990. Immunohistochemical localization of phosphoenolpyruvate carboxykinase in adult and developing mouse tissues. *J. Histochem. Cytochem.* 38:171–178.

33. Friedman, S.L., F.J. Roll, J. Boyles, and D.M. Bissell. 1985. Hepatic lipocytes: The principal collagen-producing cells of normal liver. *Proc. Natl. Acad. Sci. USA.* 82:8681–8685.

34. Casini, A., M. Pinzani, S. Milani, C. Grappone, G. Galli, A.M. Jezequel, D. Schuppan, C.M. Rotella, and C. Surrenti. 1993. Regulation of extracellular matrix synthesis by transforming growth factor β1 in human fat-storing cells. *Gastroenterology.* 105:245–253.

35. Gressner, A.M., and M.G. Bachem. 1995. Molecular mechanisms of liver fibrogenesis: a homage to the role of activated fat-storing cells. *Digestion.* 56:335–346.

36. Oberhammer, F.A., M. Pavelka, S. Sharma, R. Tiefenbacher, A.F. Purchio, W. Bursch, and R. Schulte-Hermann. 1992. Induction of apoptosis in cultured hepatocytes and in regressing liver by transforming growth factor β. *Proc. Natl. Acad. Sci. USA.* 89:5408–5412.

37. Sanderson, N., V. Factor, P. Nagy, J. Kopp, P. Kondaiah, L. Wakefield, A.B. Roberts, M.B. Sporn, and S.S. Thorgeirsson. 1995. Hepatic expression of mature transforming growth β1 in transgenic mice results in multiple tissue lesions. *Proc. Natl. Acad. Sci. USA.* 92:2572–2576.

38. Bellamy, C.O.C., R.D.G. Malcomson, D.J. Harrison, and A.H. Wyllie. 1995. Cell death in health and disease: the biology and regulation of apoptosis. *Semin. Cancer Biol.* 6:3–16.

39. Castilla, A., J. Prieto, and N. Fausto. 1991. Transforming growth factors β1 and α in chronic liver disease. Effects of interferon-α therapy. *N. Engl. J. Med.* 14:933–940.

40. Shull, M.M., I. Ormsby, A.B. Kier, S. Pawlowski, R.J. Diebold, M. Yin, R. Allen, C. Sidman, G. Proetzel, C. Galvin, et al. 1992. Targeted disruption of the mouse transforming growth factor-β1 gene results in multifocal inflammatory disease. *Nature.* 359:693–699.

41. Kulkarni, A.B., C.G. Huh, D. Becker, A. Geiser, M. Lyght, K.C. Flanders, A.B. Roberts, M.B. Sporn, J.M. Ward, and S. Karlsson. 1993. Transforming growth factor-β1 null mutation in mice causes excessive inflammatory response and early death. *Proc. Natl. Acad. Sci. USA.* 90:770–774.

42. Russell, W.E., R.J. Coffey, Jr., A.J. Ouellette, and H.L. Moses. 1988. Type β transforming growth factor reversibly inhibits the early proliferative response to partial hepatectomy in the rat. *Proc. Natl. Acad. Sci. USA.* 85:5126–5130.

43. Schackert, H.K., D. Fand, and I.J. Fidler. 1990. Transient inhibition of liver regeneration in mice by transforming growth factor β1 encapsulated in liposomes. *Cancer Commun.* 2:165–171.

44. Kopp, J.B., V.M. Factor, M. Mozes, P. Nagy, N. Sanderson, E.P. Bottinger, P.E. Klotman, and S.S. Thorgiersson. 1996. Transgenic mice with increased plasma levels of TGF-β1 develop progressive kidney disease. *Lab. Invest.* 74:991–1003.

45. Tomooka, S., W.A. Border, B.C. Marshall, and N.A. Noble. 1992. Glomerular matrix accumulation is linked to inhibition of the plasmin protease system. *Kidney Int.* 42:1462–1469.

46. Feng, L., W.W. Tang, D.J. Loskutoff, and C.B. Wilson. 1993. Dysfunction of glomerular fibrinolysis in experimental antiglomerular basement membrane antibody glomerulonephritis. *J. Am. Soc. Nephrol.* 3:1753–1764.

47. Nath, K.A. 1992. Tubulointerstitial changes as a major determinant in the progression of renal damage. *Am. J. Kid. Dis.* 20:1–17.

48. Freidman, A.L., and R.W. Chesney. 1993. Isolated renal tubular disorders. *In* Diseases of the Kidney. R.W. Schrier and C.W. Gottschalk, editors. Little, Brown and Company, Boston. 611–655.

49. Walton, G., R. Buttyan, E. Garcia-Montes, C.A. Olsson, T.W. Hensle, and I.S. Sawczuk. 1992. Renal growth factor expression during the early phase of experimental hydronephrosis. *J. Urol.* 148:510–514.

50. Border, W.A., S. Okuda, L.R. Languino, M.B. Sporn, and E. Ruoslahti. 1990. Suppression of experimental glomerulonephritis by antiserum against transforming growth factor β1. *Nature.* 346:371–374.

51. Border, W.A., N.A. Noble, T. Yamamoto, J.R. Harper, Y.U. Yamaguchi, M.D. Pierschbacher, and E. Ruoslahti. 1992. Natural inhibitor of transforming growth factor-β protects against scarring in experimental kidney disease. *Nature.* 360:361–364.

52. Akagi, Y., Y. Isaka, M. Aria, T. Kaneko, M. Takenaka, T. Moriyama, Y. Kaneda, A. Ando, Y. Orita, T. Kamada, et al. 1996. Inhibition of TGF-β1 expression by antisense oligonucleotides suppresses extracellular matrix accumulation in experimental glomerulonephritis. *Kidney Int.* 50:148–155.

53. Antonipillai, T., T. Hoang Le, L. Soceneantu, and R. Horton. 1993. Transforming growth factor-β is a renin secretagogue at picomolar concentrations. *Am. J. Physiol.* 265:F537–F541.

54. Kagami, S., W.A. Border, D.E. Miller, and N.A. Noble. 1994. Angiotensin II stimulates extracellular matrix protein synthesis through induction of transforming growth factor-β expression in rat glomerular mesangial cells. *J. Clin. Invest.* 93:2431–2437.

55. Ketteler, M., N.A. Noble, and W.A. Border. 1995. Transforming growth factor-β and angiotensin II: the missing link from glomerular hyperfiltration to glomerulo-sclerosis? *Ann. Rev. Physiol.* 57:279–295.

56. Ailhaud, G., P. Grimaldi, and R. Negrel. 1992. Cellular and molecular aspects of adipose tissue development. *Ann. Rev. Nutr.* 12:207–233.

57. MacDougald, O.A., and M.D. Lane. 1995. Transcriptional regulation of gene expression during adipocyte differentiation. *Ann. Rev. Biochem.* 64:345–373.

58. Yeh, W.C., and S.L. McKnight. 1995. Regulation of adipose maturation and energy homeostasis. *Curr. Opin. Cell Biol.* 7:885–890.

59. Torti, F.M., S.V. Torti, J.W. Larrick, and G.M. Ringold. 1989. Modulation of adipocyte differentiation by tumor necrosis factor and transforming growth factor β. *J. Cell Biol.* 108: 1105–1113.

60. Sparks, R.L., B.J. Allen, and E.E. Strauss. 1992. TGF-β blocks early but not late differentiation-specific gene expression and morphologic differentiation of 3T3 T proadipocytes. *J. Cell. Physiol.* 150:568–577.

61. Vaidya, T.B., S.J. Rhodes, E.J. Taparowsky, and S.F. Konieczny. 1989. Fibroblast growth factor and transforming growth factor β repress transcription of the myogenic regulatory gene MyoD1. *Mol. Cell. Biol.* 9:3576–3579.

62. Brennan, T.J., D.G. Edmondson, L. Li, and E.N. Olson. 1991. Transforming growth factor β represses the actions of myogenin through a mechanism independent of DNA binding. *Proc. Natl. Acad. Sci. USA.* 88:3822–3826.

63. Spiegelman, B.M., and C.A. Ginty. 1983. Fibronectin modulation of cell shape and lipogenic gene expression in 3T3-adipocytes. *Cell.* 35:657–666.

64. Kozak, L.P., U.C. Kozak, and G.T. Clarke. 1991. Abnormal brown and white fat development in transgenic mice overexpressing glycerol 3-phosphate dehydrogenase. *Genes Dev.* 5:2256–2264.

65. Foster, D.W. 1994. The lipodystrophies and other rare disorders of adipose tissue. *In* Harrison's Principles of Internal Medicine. K.J. Isselbacher, E. Braunwald, J.D. Wilson, J.B. Martin, A.S. Fauci, and D.L. Kasper, editors. McGraw-Hill Inc., New York. 2132–2136.